Geosci. Model Dev., 16, 4957–4976, 2023
https://doi.org/10.5194/gmd-16-4957-2023

Geoscientific Model Development
Open Access
EGU

Uncertainty estimation for a new exponential-filter-based long-term root-zone soil moisture dataset from Copernicus Climate Change Service (C3S) surface observations

Adam Pasik[1], **Alexander Gruber**[1], **Wolfgang Preimesberger**[1], **Domenico De Santis**[2], **and Wouter Dorigo**[1]

[1]Department of Geodesy and Geoinformation, TU Wien, Wiedner Hauptstraße 8, 1040 Vienna, Austria
[2]Research Institute for Geo-Hydrological Protection, National Research Council, Via della Madonna Alta 126, 06128 Perugia, Italy

Correspondence: Alexander Gruber (alexander.gruber@geo.tuwien.ac.at)

Received: 13 January 2023 – Discussion started: 14 March 2023
Revised: 28 June 2023 – Accepted: 30 July 2023 – Published: 31 August 2023

Abstract. Soil moisture is a key variable in monitoring climate and an important component of the hydrological, carbon, and energy cycles. Satellite products ameliorate the sparsity of field measurements but are inherently limited to observing the near-surface layer, while water available in the unobserved root-zone controls critical processes like plant water uptake and evapotranspiration. A variety of approaches exist for modelling root-zone soil moisture (RZSM), including approximating it from surface layer observations. While the number of available RZSM datasets is growing, they usually do not contain estimates of their uncertainty. In this paper we derive a long-term RZSM dataset (2002–2020) from the Copernicus Climate Change Service (C3S) surface soil moisture (SSM) COMBINED product via the exponential filter (EF) method. We identify the optimal value of the method's model parameter T, which controls the level of smoothing and delaying applied to the surface observations, by maximizing the correlation of RZSM estimates with field measurements from the International Soil Moisture Network (ISMN). Optimized T-parameter values were calculated for four soil depth layers (0–10, 10–40, 40–100, and 100–200 cm) and used to calculate a global RZSM dataset. The quality of this dataset is then globally evaluated against RZSM estimates of the ERA5-Land reanalysis. Results of the product comparison show satisfactory skill in all four layers, with the median Pearson correlation ranging from 0.54 in the topmost to 0.28 in the deepest soil layer. Temporally dynamic product uncertainties for each of the RZSM product layers are estimated by applying standard uncertainty propagation to SSM input data and by estimating structural uncertainties in the EF method from ISMN ground reference measurements taken at the surface and at varying depths. Uncertainty estimates were found to exhibit both realistic absolute magnitudes and temporal variations. The product described here is, to the best of our knowledge, the first global, long-term, uncertainty-characterized, and purely observation-based product for RZSM estimates up to 2 m depth.

1 Introduction

Soil moisture (SM) is an essential climate variable (ECV) that is crucial for understanding and modelling the Earth's climate and an important control of hydrological, energy, and carbon fluxes (GCOS, 2022; Dorigo et al., 2021a). Global monitoring of SM is necessary for a variety of applications such as meteorological modelling (Albergel et al., 2008); monitoring drought (Tobin et al., 2017); and modelling groundwater recharge (Bouaziz et al., 2020), runoff, and catchment response to storms (Brocca et al., 2010).

In situ SM measurements are considered to provide the most accurate SM data but can differ greatly in measuring equipment and usually lack estimates of their uncertainties (Dorigo et al., 2011). Widely distributed SM field measurements are available from centralized platforms such as the International Soil Moisture Network (ISMN) (Dorigo et al., 2021b). While being essential for satellite and model prod-

uct calibration and validation, in situ measurements lack the spatial coverage necessary for large-scale applications, especially in the Global South (see Fig. A1; Dorigo et al., 2021a; Mishra et al., 2020). Quasi-global SM information is available from modelled and satellite products, but their spatial resolution is very coarse (usually tens to hundreds of square kilometres) and usually insufficient to resolve the significant spatio-temporal heterogeneity of SM, which poses challenges to large-scale monitoring (Brocca et al., 2010). Global land surface model products provide gap-free and long-term SM estimates at various depths and chosen time intervals but are computationally expensive and may depend on many auxiliary inputs that are not always available globally or with sufficient quality or resolution (Mishra et al., 2020; Albergel et al., 2008). In contrast, remote sensing retrievals are available only at satellite overpass times and are unreliable under various conditions, including frozen ground, dense vegetation, and radio frequency interference (RFI) (Gruber et al., 2019; Dorigo et al., 2017). Moreover, microwaves used for SM retrieval mainly contain information on water content in the surface layer, hampering their usability for studying or modelling processes in the soil root zone. Root-zone soil moisture (RZSM), often defined as the water present in the top metre of the soil column (Mishra et al., 2020; Baldwin et al., 2017; de Lange et al., 2008), is a component of the Global Climate Observing System (GCOS) ECV portfolio and a necessary variable for closing the water cycle (GCOS, 2016, 2022). RZSM also represents the water available for plant water uptake and thus affects evapotranspiration rates (Martens et al., 2017; Ford et al., 2014; Albergel et al., 2008) and plays a critical role in agricultural productivity forecasting (Wang et al., 2017) and drought monitoring (Vreugdenhil et al., 2022; Tobin et al., 2017).

The existing link between SM dynamics in the surface layer and the root zone (Albergel et al., 2008; Wang et al., 2017; Ford et al., 2014; Sure and Dikshit, 2019) allows for the estimation of RZSM from surface SM (SSM) observations via a variety of hydrological models. These include relatively simple two-layer approaches approximating RZSM as a function of SSM (Manfreda et al., 2014), compound process-based models requiring sophisticated parameter calibration (Bouaziz et al., 2020), and immensely complex and computationally expensive land surface models requiring many auxiliary inputs (Muñoz Sabater et al., 2021; Rodell et al., 2004). Satellite-based SSM observations can also be assimilated into a land surface model to produce estimates of RZSM with global coverage, as in the case of the SMAP L4 RZSM product (Reichle et al., 2017). An alternative, less complex approach that approximates RZSM solely from SSM estimates – and can thus be readily applied to satellite retrievals – is the so-called exponential filter (EF) method (Wagner et al., 1999; Albergel et al., 2008). In essence, the EF method approximates conditions in the root zone by smoothing and delaying SSM, which is generally characterized by greater fluctuations (Beck et al., 2009; Mahmood and Hubbard, 2007). Even though the coupling strength between the surface and root-zone layers decreases with depth (Mahmood and Hubbard, 2007; Ford et al., 2014; Mishra et al., 2020), and the skill of the method in predicting RZSM has been demonstrated to deteriorate accordingly (Paulik et al., 2014; Brocca et al., 2010; Sure and Dikshit, 2019), it is still widely used due to its relatively good performance and independence of ancillary inputs as well as its low computational cost and overall simplicity. However, the EF method is susceptible to prolonged data gaps in SSM data and thus requires an adequate number of input observations within a time interval consistent with the temporal scale of RZSM dynamics.

Regardless of the method used to derive RZSM estimates, most products do not provide information about the magnitude of random errors such as the standard deviation of their distribution, hereinafter referred to as uncertainties (Gruber et al., 2020). Two approaches have been proposed to characterize the time-variant quality of RZSM estimates derived with the EF method. The first approach, reported in Bauer Marschallinger (2018) and also utilized in this study, is a quality flag that is derived from the number of valid SSM estimates available within a specific time window preceding a specific EF-based RZSM estimate. The second approach, proposed by De Santis and Biondi (2018), uses the standard law of uncertainty propagation (Taylor, 1997) in order to characterize the random error variances of EF-based RZSM estimates. This approach takes into account the uncertainties in both the SSM input data and the EF model parameter but does not consider the model structural error in the EF method (Beven, 2005). The latter, due to the simplistic nature of the EF method and the limited surface–root-zone coupling, can also contribute significantly to the uncertainty budget and thus must not be neglected when characterizing product errors.

In this paper, we propose to estimate the model structural uncertainty in the EF using in situ measurements of surface and root-zone SM from the ISMN. We then use these estimates together with the law for the propagation of uncertainties (similar to De Santis and Biondi, 2018) to produce a global, fully error-characterized RZSM dataset for four soil layers (0–10, 10–40, 40–100, and 100–200 cm) between 2002 and 2020, taking C3S soil moisture as input to the model. While other EF-based datasets exist (e.g. the SMOS L4 product), they offer limited spatio-temporal coverage and lack quantitative uncertainty information (Al Bitar and Mahmoodi, 2020; Bauer-Marschallinger et al., 2018). The focus and novelty of this paper are in quantifying, rather than reducing, the EF model's known limitations by providing methodology for comprehensive uncertainty estimation for the EF method. Additionally, to the best of our knowledge, our dataset is, as yet, the longest available observation-based, error-characterized global RZSM product.

2 Datasets and data pre-processing

2.1 C3S surface soil moisture

Global input satellite surface observations were obtained from the Copernicus Climate Change Service (C3S) surface soil moisture COMBINED product v202012, hereinafter referred to as C3S SSM. C3S SSM is a merged product that combines satellite SSM retrievals from 4 active and 10 passive microwave sensors into a daily global dataset on a regular 0.25° grid, expressed in volumetric units ($m^3\ m^{-3}$) (C3S, 2020). Invalid retrievals due to frozen ground, dense vegetation, RFI, and other factors are masked out. Although the C3S product provides SSM data from 1978 onward, their quality and spatio-temporal coverage have increased significantly in more recent periods, when sensors measuring in frequency domains better suitable for SSM retrieval became available. Therefore, only C3S SSM data for the period 2001–2020 were used in this study. Note that data from the first year of this period were used only as the model adjustment period and not included in later analyses.

The uncertainty estimates provided for the merged SSM retrievals in the C3S SSM product were computed by means of triple collocation analysis (TCA) (Gruber et al., 2017). More specifically, (stationary) uncertainties were estimated for each satellite sensor separately and used to calculate the merging weights. Uncertainties in the merged SSM estimates were then calculated from the law for the propagation of uncertainties to account for the quality improvement due to the merging. Note that the distinctive life spans of the satellite missions therefore also lead to distinctive changes in the data quality of the merged product. These sudden changes in product uncertainty are hereinafter referred to as structural breaks (Preimesberger et al., 2021). As more and newer sensors provide better-quality retrievals, mean uncertainty values after each structural break typically decrease (Gruber et al., 2017). This is apparent, for example, in the shift in C3S SSM uncertainty values after the introduction of AMSR-E in 2002 (van der Schalie et al., 2017; Gruber et al., 2019).

C3S data are readily available from the Copernicus Climate Data Store (CDS), and detailed information on the C3S dataset and its underlying ESA CCI v5 merging algorithm can be found in the relevant documentation (C3S, 2020; Dorigo et al., 2021c).

2.2 Soil moisture field measurements

Field measurements for optimizing the model parameters of the EF method and for estimating its uncertainties were obtained from the International Soil Moisture Network (ISMN) for the period 2002–2020 (Dorigo et al., 2021b). Only data from sensors with a measuring depth ≤ 200 cm and internally flagged as reliable (Dorigo et al., 2013) were considered. Measuring depths of SM sensors placed vertically in a depth range, e.g. 10–40 cm, refer to their mean measuring depth. Data from multiple sensors installed at the same location and depth were averaged. ISMN data, typically available as hourly readings, were aggregated to mean daily values to match the temporal sampling of satellite observations. Furthermore, we only used ISMN stations where at least 100 data points concurrent with C3S SSM retrievals were available. Notably, approximately 80 % of the selected ISMN time series originate from North America and Europe (Fig. A1), and the availability of data declines with depth.

2.3 ERA5-Land soil moisture

ERA5-Land (E5L) is a multi-decadal climate reanalysis with an extensive portfolio of land variables computed by the assimilation of ERA5 atmospheric variables into the H-TESSEL land surface model (Muñoz Sabater et al., 2021). Modelled SM data are available for four depth layers (0–7, 7–28, 28–100, and 100–289 cm) on a regular 0.1° grid and are accessible via the Copernicus Climate Data Store (CDS) (Muñoz Sabater, 2019, 2021). We used E5L for a product intercomparison with the RZSM product developed in this study, carried out for the period 2002–2020 within the Quality Assurance for Soil Moisture framework (QA4SM; https://qa4sm.eu, last access: 28 August 2023), which automatically resamples and matches observations of the compared datasets and delivers a wide range of validation metrics.

3 Methods

3.1 Exponential filter

The EF method (Wagner et al., 1999) relies on a simple two-layer water balance model where the only considered exchange between the surface layer and the reservoir below it is infiltration. The method assumes that the fluxes from the surface to the sub-surface layers are proportionate to the difference in SM content between both layers. In this study, we utilize the recursive formulation of the method (Albergel et al., 2008):

$$\mathrm{RZSM}(t_n) = \mathrm{RZSM}(t_{n-1}) + K_n \cdot (\mathrm{SSM}(t_n) - \mathrm{RZSM}(t_{n-1})), \quad (1)$$

where t_n and t_{n-1} denote timestamps (in days) of the current and previous SSM observations, respectively. Conditions in the root zone are approximated by a weighted combination of the new input SSM observation and past model estimates, with more recent estimates receiving higher weights on a timescale defined by the method's only parameter T (temporal length, typically in days). Weights are controlled by the gain term K, which ranges from 0 to 1 and is calculated as follows:

$$K_n = \frac{K_{n-1}}{K_{n-1} + \mathrm{e}^{-\frac{t_n - t_{n-1}}{T}}}. \quad (2)$$

At initialization, when no preceding estimates are available, the EF calculation is started with $K_0 = 1$ and $\mathrm{RZSM}(t_0) = \mathrm{SSM}(t_0)$.

Temporal variability in the root zone is generally smaller than at the surface; hence the T value and its associated level of smoothing applied to the SSM data increase with depth (Wagner et al., 1999; Paulik et al., 2014; Wang et al., 2017; Beck et al., 2009; Mahmood and Hubbard, 2007). The optimal T value (T_{opt}, the value that leads to the best possible representation of RZSM at a certain location using the EF) has been related to differences in utilized SSM sensors (Bouaziz et al., 2020; Sure and Dikshit, 2019), SSM sampling frequency (Brocca et al., 2010; Pellarin et al., 2006), and land surface features (Albergel et al., 2008; de Lange et al., 2008). In particular, T acts as a conglomerate proxy for various environmental factors assumed to govern the infiltration process (e.g. soil texture, evapotranspiration, and climate), but past research on the importance of the exact driving factors is inconclusive and even contradictory (Wang et al., 2017; Bouaziz et al., 2020). To optimize the T parameter, numerous control factors have been tested (Bouaziz et al., 2020; Mishra et al., 2020; Stefan et al., 2021), and ever more sophisticated methods have been employed, including machine learning approaches (Grillakis et al., 2021). Other limitations of the method include generally poorer performance in arid zones and when soil texture is not homogeneous throughout the soil column (Ford et al., 2014; Yang et al., 2022).

Due to the high spatio-temporal heterogeneity of SM (Famiglietti et al., 2008) and its surface–root-zone coupling – and hence the difficulty in properly estimating the T parameter accurately – an uncalibrated value of $T = 20$ has sometimes been used to describe all of the water content in the first 100 cm of the soil column (Wagner et al., 1999; de Lange et al., 2008). Results obtained by using a constant value $T = 20$ were similar to those obtained with T values calibrated for soil texture (de Lange et al., 2008). Limited sensitivity of the EF to T due to different environmental factors was also observed by other studies, which supports choosing a single value for T_{opt} to represent a particular depth for large areas or even globally (Albergel et al., 2008; Brocca et al., 2010, 2011; Grillakis et al., 2021).

3.1.1 RZSM quality flags

Prolonged temporal data gaps will cause K to increase and may cause the EF to put excessive weight on new SSM input. In the extreme case, a very long data gap (whose duration depends on the chosen T value) can reset the EF to the initial state of $K_n = 1$ and $\mathrm{RZSM}(t_n) = \mathrm{SSM}(t_n)$ (see above). We run a 1-year adjustment period (2001) for K to reach an equilibrium state and utilize the EF quality flag (qflag) described in Bauer Marschallinger (2018) to avoid such reinitializations due to frequent and/or persistent data gaps. The qflag is recursively calculated for each RZSM estimate and reflects the availability of SSM input data in the preceding time period.

$$\mathrm{qflag}(t_n) = \begin{cases} 1 + \mathrm{qflag}(t_{n-1}) \cdot e^{-\frac{t_n - t_{n-1}}{T}}, & \text{if SSM at } t_n \text{ is available} \\ \mathrm{qflag}(t_{n-1}) \cdot e^{-\frac{t_n - t_{n-1}}{T}}, & \text{if SSM at } t_n \text{ is unavailable} \end{cases} \quad (3)$$

The quality flag calculation is initialized with $\mathrm{qflag}(t_n) = 1$. A normalization factor of $\sum_{j=0}^{\infty} \mathrm{e}^{-\frac{j}{T}}$ is used to express the calculated flag values in percentages, with higher values indicating a greater density of SSM data available for calculation. If the quality flag falls below a T-specific threshold, RZSM estimates are masked out. The thresholds used here have been interpolated from those empirically determined by Bauer Marschallinger (2022) for a set of discrete T values (35 %, 40 %, 45 %, 50 %, 55 %, 60 %, 65 %, and 70 % for the T values 2, 5, 10, 15, 20, 40, 60, and 100, respectively). If input data are unavailable, but satisfactory data density has been achieved in the preceding days, the latest RZSM estimate is propagated forward until new input data become available, or the quality flag drops below its respective threshold. In the latter case, the output value is masked out. Importantly, even if new SSM input becomes available to the EF after prolonged data gaps, RZSM estimates derived from it remain masked until the qflag exceeds the aforementioned threshold again.

3.1.2 T-parameter optimization

We optimize T for a particular depth of the soil column by maximizing the correlation between the satellite-based RZSM estimates and the in situ measurements (Paulik et al., 2014; Grillakis et al., 2021). Satellite and in situ data are matched in space by means of the nearest-neighbour method. The impact of the spatial mismatch error between the large footprint of the satellite-based product and point-scale field measurement is mitigated by excluding time series that exhibit a correlation coefficient (Pearson's r) lower than 0.5 (Grillakis et al., 2021) or that are not statistically significant ($p \geq 0.05$).

EF calculations are repeated for T values of 1–100, and T_{opt} is selected for each of the available ISMN time series based on the highest correlation coefficient. We then group T_{opt} values based on the measurement depth of the respective in situ sensor into four bins corresponding to the RZSM target layers. These depth layers, chosen to be 0–10, 10–40, 40–100, and 100–200 cm, were defined to reflect those in common model-based RZSM products (Rodell et al., 2004; Muñoz Sabater et al., 2021). Finally, the median value of T_{opt} from each bin is chosen to compute a global RZSM product from the C3S SSM dataset.

A cross-validation is carried out to verify that T_{opt} values were not over-fitted to the local ISMN site conditions. Therefore, the sample set is randomly divided into five subsets of

equal size (per bin), and then each of the subsets was used once to validate the method fit to the remaining four bins.

3.2 Uncertainty estimation

3.2.1 Baseline method

In De Santis and Biondi (2018), the standard law for the propagation of uncertainties is applied to the EF method. We use this approach as a baseline for our analyses. The recursive formulation of this baseline method is as follows:

$$\sigma(\mathrm{RZSM}_n) = \sqrt{\Delta_n^2 + \left(\frac{\partial \mathrm{RZSM}_n}{\partial T}\right)^2 \sigma^2(T)}, \tag{4}$$

where

$$\Delta_n^2 = K_n^2 \sigma^2(\mathrm{SSM}_n) + (1 - K_n)^2 \Delta_{n-1}^2, \tag{5}$$

and

$$\frac{\partial \mathrm{RZSM}_n}{\partial T} = \frac{K_n}{T}\left[G_n(\mathrm{RZSM}_{n-1} - \mathrm{RZSM}_n) + e^{-\frac{t_n - t_{n-1}}{T}} \frac{T}{K_{n-1}} \frac{\partial \mathrm{RZSM}_{n-1}}{\partial T}\right], \tag{6}$$

with G_n defined as

$$G_n = e^{-\frac{t_n - t_{n-1}}{T}}\left(G_{n-1} + \frac{1}{K_{n-1}} \frac{t_n - t_{n-1}}{T}\right). \tag{7}$$

$\sigma(\mathrm{RZSM})$ and $\sigma(T)$ denote the uncertainty in the RZSM estimates and the EF model parameter T, respectively. The equation is initialized as $\Delta_0 = \sigma(\mathrm{SSM}_0)$, $\partial \mathrm{RZSM}_0/\partial T = 0$, and $G_0 = 0$. Uncertainties in the SSM input data are considered by the Δ term, which also takes into account the effect of possible prolonged input data gaps dependent on the T value. The Jacobian term $\partial \mathrm{RZSM}/\partial T$ assumes high values proportional to the latest SSM input variability on a timescale related to the T parameter. This is reflected in significant changes in the RZSM value associated with wetting or drying of the soil.

3.2.2 T-parameter uncertainty

De Santis and Biondi (2018) used an arbitrary value of $\sigma(T)$ equal to 10 % of locally calibrated T_{opt}. This is in line with other studies on SM uncertainty propagation (Parinussa et al., 2011; Pathe et al., 2009), who used this uncertainty percentage for parameters without well-defined accuracy. In our study, we determine T_{opt} values based on a limited number of available in situ time series and apply these values to estimate RZSM globally. Consequently, $\sigma(T)$ is likely to be greater due to a variety of environmental conditions not accounted for or underrepresented in the available in situ sample. We therefore propose the median absolute deviation (MAD) of T_{opt} (Sect. 3.1.2) as a more appropriate proxy for $\sigma(T)$. In this case, the MAD is preferred over the variance because the sampling distribution of T_{opt} is both non-Gaussian and bounded (Leys et al., 2013).

3.2.3 EF model structural uncertainty

Recall that the standard law for the propagation of uncertainty (which is used in the baseline method) does not account for model structural uncertainty in the EF, which, due to the simplistic nature of the method and the limited surface–root-zone coupling, can account for a significant portion of the overall uncertainty budget.

We propose to estimate model structural uncertainty ($\sigma(\mathrm{EF})$) from in situ data using stations that operate sensors both at the surface and in the root zone. At these stations, we derive RZSM estimates from the SSM measurements using the EF method and then compare them to actual RZSM station measurements. For this analysis, the T value was optimized for each station and depth individually to minimize its influence on the estimation of $\sigma(\mathrm{EF})$. This provides direct estimates for $\sigma(\mathrm{EF})$ as

$$\sigma(\mathrm{EF}) = \mathrm{ubRMSD}(\mathrm{RZSM}_{\mathrm{EF}}, \mathrm{RZSM}_{\mathrm{ISMN}}), \tag{8}$$

where ubRMSD denotes the unbiased root-mean-square difference. Note that "unbiased", in this case, refers not only to a correction for bias in the mean (as is most commonly done) but also to a correction for bias in variance, which also constitutes an unintended systematic component in the RMSE (Gupta et al., 2009). Only sites with measurements from more than a single depth and at least one sensor within the surface layer (≤ 10 cm) were selected. Time series with negative correlation between EF-based RZSM estimates and in situ RZSM measurements were disregarded. As a result, a total of 1509 in situ sites were considered. Note that the EF model structural uncertainty computed at the point scale is assumed to be representative of the coarse scale as well.

Finally, the EF structural uncertainties obtained from Eq. (8) add to the propagated RZSM uncertainty budget (Eq. 4) as

$$\sigma(\mathrm{RZSM}_n) = \sqrt{\Delta_n^2 + \left(\frac{\partial \mathrm{RZSM}_n}{\partial T}\right)^2 \sigma^2(T) + \sigma^2(\mathrm{EF})}. \tag{9}$$

4 Results and discussion

In this section, we first show results of the T-parameter point-scale optimization. Next, we compare the gridded RZSM product globally to E5L. We then discuss the estimates for EF model structural uncertainties. Finally, we compare our RZSM uncertainty estimates with those obtained with the baseline method.

4.1 T-parameter optimization

After filtering out unreliable data (see Sect. 2.2), 3901 ISMN time series from 67 different measuring depths between 0 and 200 cm were available for the T-optimization process. Figure 1 shows the distribution of T_{opt} values binned into our

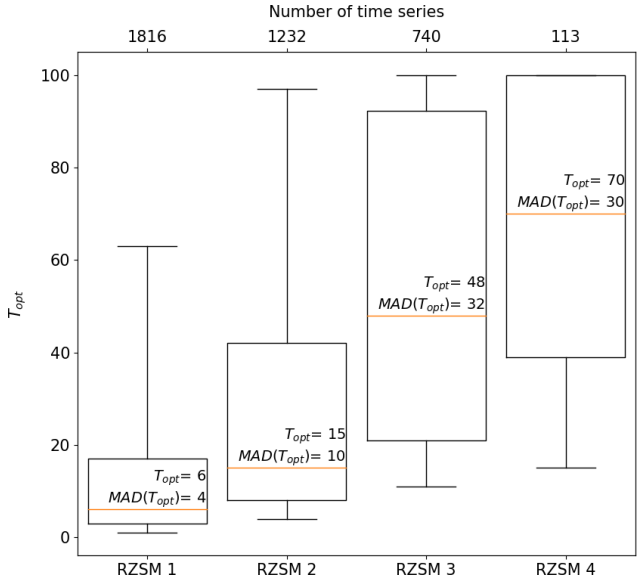

Figure 1. T_{opt} values calibrated with 3901 in situ time series and binned according to RZSM layers 1–4. Median values (represented by orange lines) from each bin were used to compute a global RZSM product. Median absolute deviations (MAD(T_{opt})) were used to estimate RZSM uncertainties.

four chosen RZSM layers (0–10, 10–40, 40–100, and 100–200 cm). The median T_{opt} values for these layers were 6, 15, 48, and 70 d, increasing with soil depth as expected (Paulik et al., 2014; Wang et al., 2017). These median T_{opt} values were then used to compute RZSM globally.

A fivefold cross-validation was performed to verify the robustness of this approach. The variability in median T_{opt} values per soil layer increases with depth but remains negligibly small in all layers, with 6, 15–16, 47–50, and 67–72 for soil layers 1–4, respectively (Fig. 2a). Subsequently, the five median T_{opt} values derived from the training subsets were used to estimate RZSM for the different layers of the respective validation sets (Fig. 2c) and resulted in Pearson's r of 0.64–0.67, 0.64–0.65, 0.57–0.6, and 0.48–0.6 for soil layers 1–4, respectively. When evaluating each training set directly, correlations were 0.65–0.66, 0.65, 0.58–0.59, and 0.53–0.56 for soil layers 1–4, respectively (Fig. 2b).

The little variability between the validation and training sets suggests that T_{opt} values are not over-fitted to ISMN site conditions and can be used robustly in other regions as well. Notably, the spread in median T_{opt} values increases with soil depth, while the correlation scores decrease. This indicates reduced reliability of the method in deeper soil layers, which is in line with the assumption that the coupling between the surface and root-zone SM decreases with depth. Note, however, that results for deeper layers are also affected by the smaller sample sizes at greater depths.

4.2 Global RZSM product quality assessment

A global SM dataset spanning the period 2002–2020 was computed using the EF method and T parameters optimized at point-scale with the approach described in Sect. 4.1. Figure 3a–e show correlation maps of each of the RZSM product layers as well as the input C3S SSM dataset with E5L; median correlation coefficients are summarized in Fig. 3f.

The spatial patterns observed in the C3S SSM data (Fig. 3a) are strikingly similar in RZSM layer 1 (Fig. 3b), with observed slight to moderate deterioration in performance over the high latitudes ($> 60°$ N). This is not surprising given that both products differ only by a small degree of smoothing applied to RZSM layer 1 and are compared to the same E5L layer (0–7 cm). RZSM layers 2 and 3 (Fig. 3c–d), respectively, are compared to E5L layers 7–28 and 28–100 cm, respectively, and largely preserve good performance in regions where the input C3S SSM product also performs well, i.e. Europe (bar Scandinavia), the Caspian and Aral sea basins, the eastern United States, India, Southeast Asia, South America, sub-Saharan Africa, and Australia. At the same time deterioration of performance is observed at high latitudes and in arid environments such as the Sahara desert and the Arabian Peninsula, where the reduced strength of coupling between the surface and root-zone dynamics hinders the EF performance (Yang et al., 2022). Areas of good and poor performance visible in RZSM layers 1–3 are not apparent in RZSM layer 4 (Fig. 3e), where agreement with the reference E5L is very heterogeneous. A few regions where the good performance observed in shallower layers was preserved are India, Southeast Asia, and the eastern United States.

The median Pearson correlations between the RZSM product and the E5L reference layers (0–7, 7–28, 28–100, and 100–289 cm) were 0.54 (RZSM layer 1), 0.47 (RZSM layer 2), 0.41 (RZSM layer 3), and 0.28 (RZSM layer 4), respectively (Fig. 3f). The C3S SSM data included in this comparison show only marginally better performance against the E5L reference (0–7 cm) than the RZSM layer 1, with a median Pearson correlations of 0.55 and 0.54, respectively.

The results are also consistent with the assumption of the EF model that SM dynamics decrease with depth and that T_{opt} ought to increase accordingly, as was also found by other studies (Wagner et al., 1999; Paulik et al., 2014; Wang et al., 2017; Beck et al., 2009; Mahmood and Hubbard, 2007). At the same time, the maximum correlation values decrease with depth, confirming the diminishing coupling between the surface and root-zone layers, as also found at the in situ station level (Fig. 2) and demonstrated by others (Paulik et al., 2014; Brocca et al., 2010; Sure and Dikshit, 2019).

4.3 EF model structural uncertainty

Figure 4 shows estimates for the model structural uncertainties (Sect. 3.2.3) obtained at all available in situ sites, binned

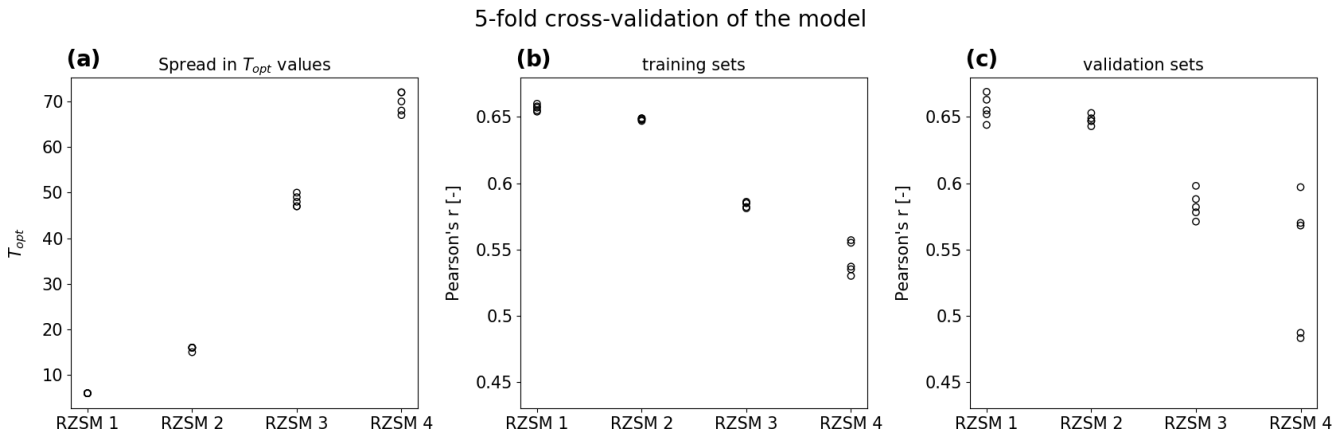

Figure 2. Cross validation results showing the spread in T_{opt} values **(a)** and agreement of the training **(b)** and validation **(c)** sets with in situ data.

into the four RZSM product layers. Their median values (represented by orange lines and annotated) were used as estimates for $\sigma(\mathrm{EF})$. Note that in situ measurement errors were assumed to be negligible and thus did not influence ubRMSD estimates, which likely causes model structural uncertainties to be overestimated. Also, structural uncertainties are assumed to be constant in time.

As anticipated, an increase in $\sigma(\mathrm{EF})$ corresponds to the growing distance between the surface and the root-zone measurements, demonstrating the decreasing coupling strength between both layers. Note that $\sigma(\mathrm{EF})$ shows significant variability within RZSM layers, which is likely, at least to some degree, related to variations in local conditions. However, as with the T-parameter optimization, we estimate structural uncertainties based only on a limited number of in situ stations and therefore use the median to extrapolate globally.

4.4 RZSM uncertainty budget calculation

Figure 5 compares RZSM uncertainty estimates obtained from the baseline method (De Santis and Biondi, 2018) with those from the approach proposed here. Figure 5a shows a time series of RZSM uncertainties from the baseline method at an arbitrary location. Figure 5b shows the effect of changing $\sigma(T)$ from 10 % of T_{opt} to the median absolute deviation of T_{opt}, which is an amplified temporal variability. Simultaneously, mean uncertainty values increase and become closer to the magnitudes of the input SSM dataset. Moreover, they no longer diminish with increasing T values (i.e. depth), as is the case in the baseline formulation. This is presumably more realistic since the progressive decoupling between the surface and deeper soil layers can be expected to cause uncertainties to increase rather than to decrease.

Figure 5c shows the impact of accounting for $\sigma(\mathrm{EF})$ in the total uncertainty budget when using 10 % of T_{opt} as the T-parameter uncertainty ($\sigma(T)$). Considering this term substantially increases the magnitude of the propagated uncertainties and leads them to increase with depth (as does $\sigma(\mathrm{EF})$). However, the uncertainties' temporal variability is reduced substantially as the effect of $\sigma(T)$ is overshadowed by that of $\sigma(\mathrm{EF})$. Finally, Fig. 5d shows the combined effect of using the MAD of T_{opt} as its parameter noise $\sigma(T)$ and accounting for model structural uncertainty $\sigma(\mathrm{EF})$. Compared to the baseline (Fig. 5a), this yields an increased overall magnitude of the uncertainties; a more realistic increase in (temporal average) uncertainties with depth; and an amplified temporal variability in all layers during transitions between dry and wet conditions, which is also expected (see Fig. 6).

4.5 Assessment of uncertainty estimates

Similar to De Santis and Biondi (2018), we assess the use of the proposed MAD estimates for $\sigma(T)$ by computing Pearson's r and root-mean-square differences (RMSDs) with respect to in situ data before and after removing a fixed percentage of the data (5 %, 10 %, 15 %, and 20 %) with the highest uncertainty estimates. In the case of effective correspondence between high values of both the estimated RZSM uncertainties and the observed RZSM deviations from reference in situ measurements, it is expected that the skill metrics will improve due to the masking. This hypothesized correspondence holds well as long as the difference between in situ and satellite-based RZSM values is mainly due to the random errors in the latter. Note that this analysis is only sensitive to the impact of using different values for $\sigma^2(T)$ ($(T_{\mathrm{opt}}/10)^2$ versus $\mathrm{MAD}(T_{\mathrm{opt}})^2$) since the estimated structural uncertainty $\sigma(\mathrm{EF})$ is constant in time and therefore cannot change the ranking of the total uncertainties.

Figure 6a and d indicate (in magenta shading) 20 % of RZSM layer 2 data with the highest uncertainties masked out in the experiment described above, based on uncertainties estimated with the baseline (b) and our method (d), respectively. Overall, despite the differences in magnitude and amplitude, both our and the baseline method assign the high-

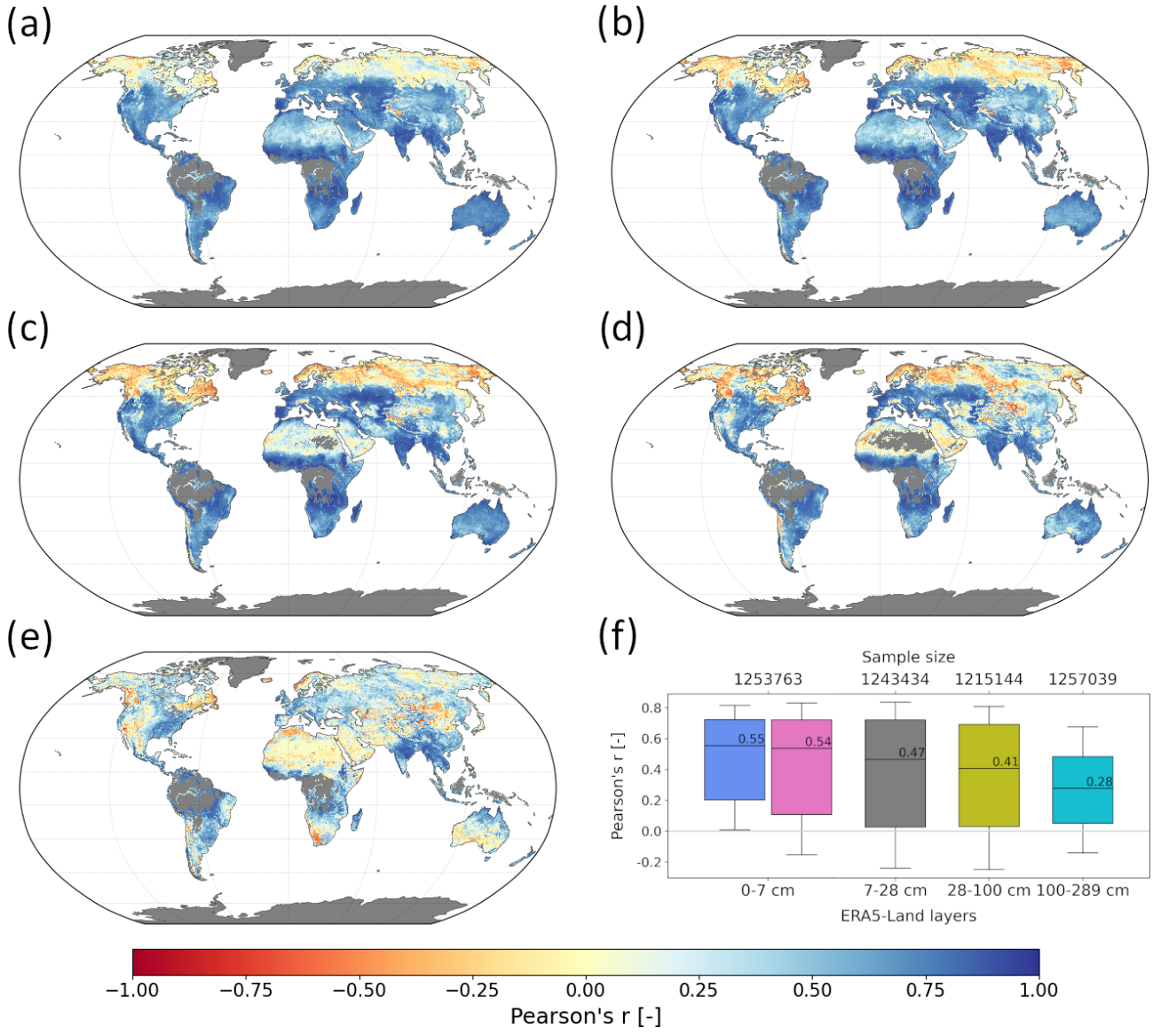

Figure 3. Spatial correlation maps of the C3S SSM and RZSM products with E5L SM **(a–e)**.

est uncertainty values to timestamps corresponding to significant soil wetting or drying events. However, with the baseline method the average magnitude of SSM input uncertainty appears to have a greater influence on the calculated RZSM uncertainty estimates. This is most evident when comparing values before and after the inclusion of Metop-A ASCAT into the C3S product in January 2007 (indicated by the dashed vertical line in Fig. 6), which substantially improved data quality thereafter. Specifically, the mean C3S SSM uncertainty dropped from 0.029 to 0.018 $m^3\ m^{-3}$. Such a clear shift is also visible in the uncertainty values propagated with the baseline method (from 0.008 $m^3\ m^{-3}$ before to 0.004 $m^3\ m^{-3}$ after the introduction of Metop-A ASCAT). This causes the baseline method to predict that the majority of the 20 % most uncertain SM values will occur in the pre-ASCAT period. In contrast, in our approach, average uncertainties remain stable (at 0.036 $m^3\ m^{-3}$) over the entire time period. This suggests that the use of $\mathrm{MAD}(T_{\mathrm{opt}})^2$ as an estimate for T-parameter uncertainty reduces the sensitivity to structural breaks, i.e. large variations between the uncertainties in the C3S SSM input sensors, and improves the method's capability to predict day-to-day uncertainty variations. Lastly, after the introduction of ASCAT, both schemes consistently assign higher uncertainties to timestamps characterized by large SM changes. Taken together, while the use of $T_{\mathrm{opt}}/10$ as the T-parameter uncertainty seems to yield realistic estimates for uncertainty variations due to the use of different C3S SSM input sensors, using $\mathrm{MAD}(T_{\mathrm{opt}})$ as the T-parameter uncertainty seems to better predict day-to-day uncertainty variations in the RZSM estimates.

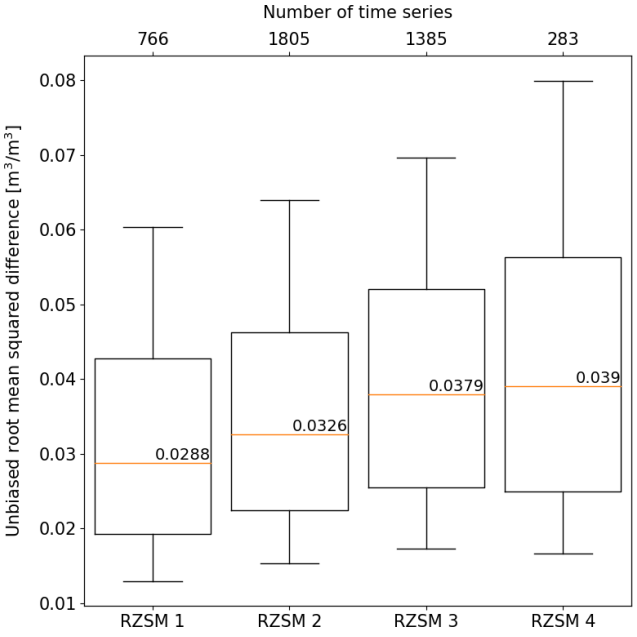

Figure 4. The ubRMSD between propagated RZSM from in situ SSM using the EF model and measurements of RZSM at the same location and the same depth, calculated at 1509 different sites. The median ubRMSD value for each bin (represented by orange lines and annotated) represents σ(EF) for the respective T_{opt}.

Figure 7 shows the results of the data removal experiment described above, summarized for all considered ISMN stations. To compare the performance with and without the effect of C3S structural breaks on the uncertainty values (see above), results are shown for both the full product period (2002–2020; Fig. 7a–d) and a sub-period without breaks, i.e. from the inclusion of SMAP data onward (1 April 2015–2020; Fig. 7e–h). In both cases, correlation coefficients obtained for the complete time series were compared to those obtained after removing 5 %, 10 %, 15 %, and 20 % of data with the highest associated uncertainties.

In the case of the full product period (Fig. 7a–d), using $\sigma(T) = T_{\mathrm{opt}}/10$ as the T-parameter uncertainty seems to consistently yield more realistic estimates of temporal uncertainty variations than using $\sigma(T) = \mathrm{MAD}(T_{\mathrm{opt}})$. This is true for all four soil layers. Masking out more uncertain data indicated by either method consistently improves agreement with in situ reference data in the first two product layers. This improvement increases the more data are masked out, as is expected. In the absence of such breaks (Fig. 7e–h) RZSM uncertainty variations seem to be better predicted when using $\sigma(T) = \mathrm{MAD}(T_{\mathrm{opt}})$ as the T-parameter uncertainty in almost all cases. Notably, in layers 3 and 4, data removal according to either method degraded the agreement with field measurements.

In summary, the propagation of C3S SSM input uncertainties yields accurate predictions of temporal uncertainty variations in RZSM estimates obtained with the EF method for the first two layers (0–10 and 10–40 cm). This is no longer the case for deeper layers (40–100 and 100-200 cm). Note, however, that the RZSM estimates in these layers themselves still exhibit reasonable skill when evaluated against E5L (see Fig. 3).

5 Summary and conclusions

In this study, we computed root-zone soil moisture (RZSM) globally in four depth layers (0–10, 10–40, 40–100, and 100-200 cm) from merged satellite surface soil moisture (SSM) retrievals of the Copernicus Climate Change Service (C3S) COMBINED product v202012 using the exponential filter (EF) method. The EF model parameter T has been optimized at point scale by maximizing the correlation with globally distributed in situ SM measurements from the International Soil Moisture Network (ISMN). The medians of the optimized T values at each layer have been used to compute the global product. A global product intercomparison with ERA5-Land (E5L) reanalysis SM data has shown a satisfactory level of agreement in all layers (global median correlations of the four above-mentioned product layers against E5L reference layers 0–7, 7–28, 28-100, and 100-289 cm were 0.54, 0.47, 0.41, and 0.28, respectively).

Uncertainties in the RZSM estimates obtained with the EF method were calculated using the law for the propagation of uncertainties. Uncertainties in the input SSM data were available in the C3S product and have been calculated by the data producers using triple collocation analysis (TCA). We tested the use of the median absolute deviation of optimized T parameters at the available ISMN locations ($\mathrm{MAD}(T_{\mathrm{opt}})$) as a proxy for T-parameter noise. Results obtained using $\mathrm{MAD}(T_{\mathrm{opt}})$ in uncertainty propagation were compared with results obtained using 10 % of the optimized T parameter itself ($T_{\mathrm{opt}}/10$), as done in earlier studies. While the use of $T_{\mathrm{opt}}/10$ as the T-parameter uncertainty seems to yield realistic estimates for uncertainty variations due to the use of different C3S SSM input sensors, using $\mathrm{MAD}(T_{\mathrm{opt}})$ as the T-parameter uncertainty seems to better predict day-to-day uncertainty variations in the RZSM estimates.

Even though propagating SSM input and model parameter uncertainties yields credible predictions of temporal uncertainty variations, absolute uncertainty magnitudes appear unrealistically small (below 0.01 $\mathrm{m^3\,m^{-3}}$). This is because the propagation of uncertainty only accounts for uncertainties in the data and parameters input to the EF method, but not for limitations of the EF method itself (e.g. the progressive inability of the method to model deeper-layer RZSM due to vanishing surface–root-zone coupling). We proposed to estimate these EF model structural uncertainties as the unbiased root-mean-square differences between RZSM estimates for each of our four product depth layers obtained by applying the EF method to in situ SSM measurements and actual

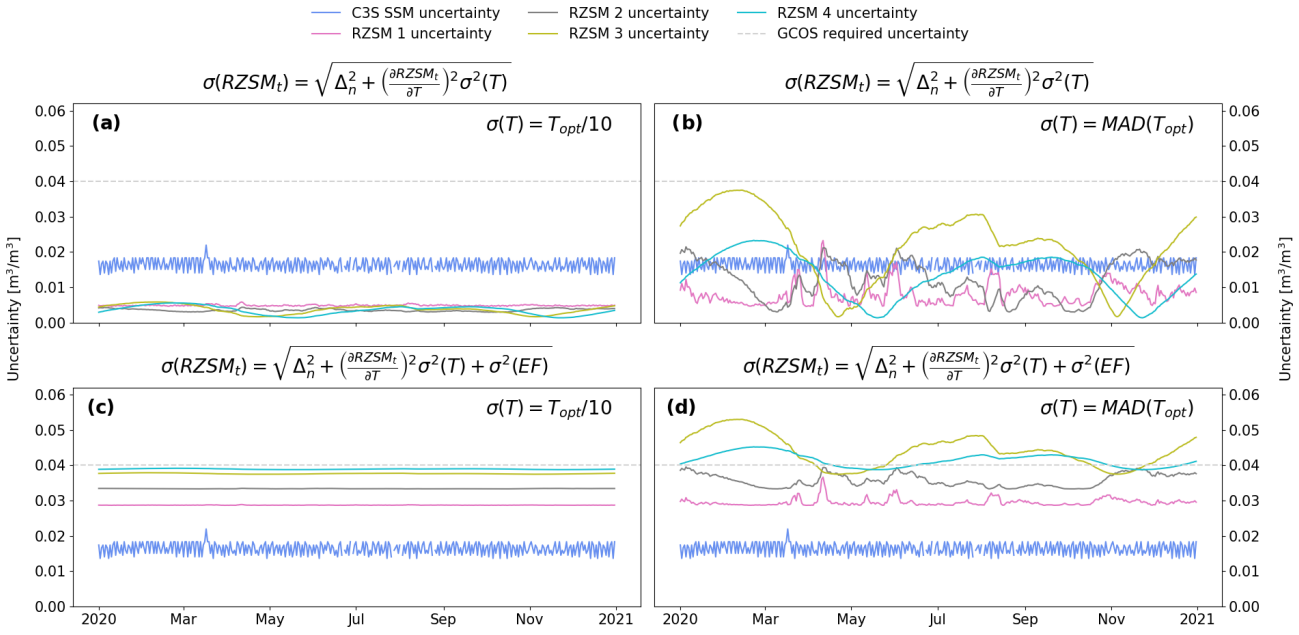

Figure 5. Evaluation of the impact of changes to the baseline method illustrated using an example 2020 time series from 9.875° N, 1.625° E. C3S SSM uncertainties were propagated with the baseline scheme in **(a)**, while **(b)** and **(c)** show the individual impacts of increasing the noise of T from 10 % of T_{opt} to MAD(T_{opt}) and adding the term σ^2(EF), respectively. Combined effects of both changes are shown in **(d)**. The dashed grey line indicates the uncertainty level defined by GCOS (2022) as an accuracy goal for RZSM products.

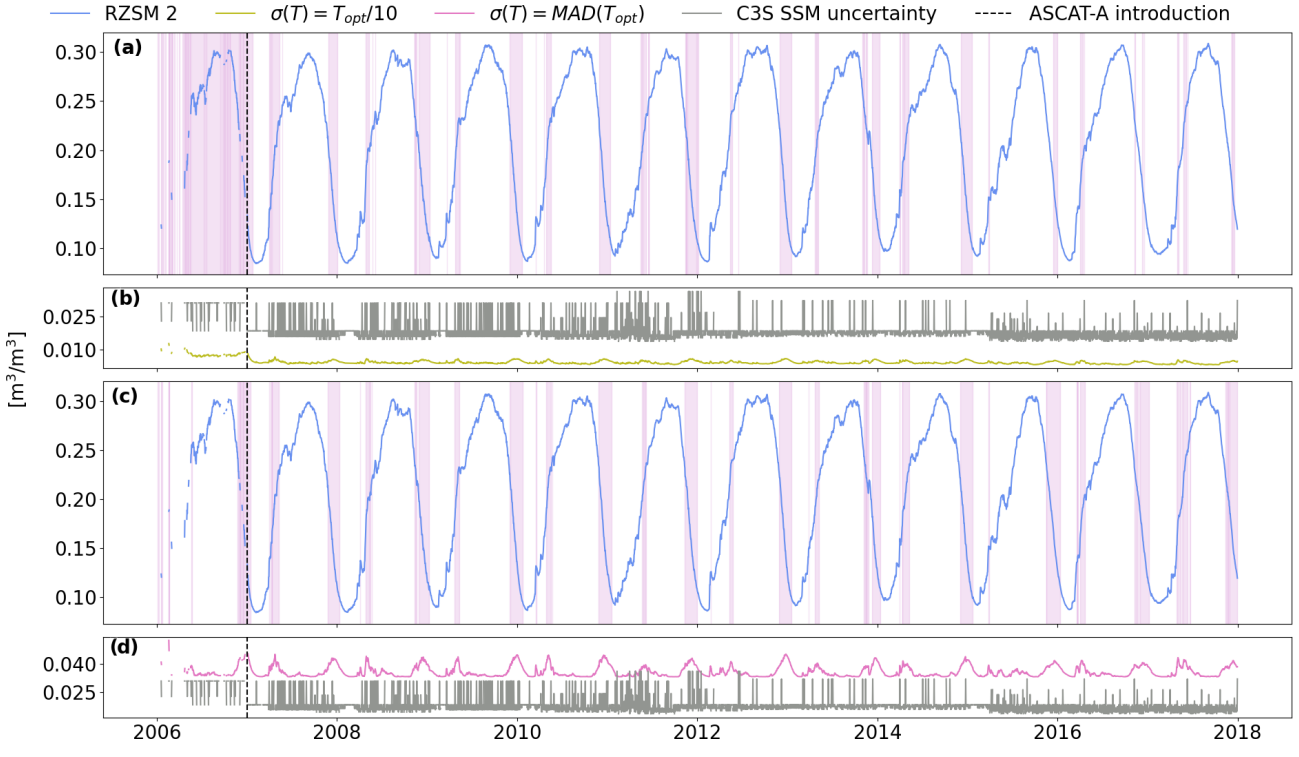

Figure 6. Differences in uncertainty variations in the baseline **(a–b)** and our proposed uncertainty estimation approach **(c–d)**. Illustrated using the example of RZSM layer 2 at an arbitrary location in Benin (9.875° N, 1.625° E).

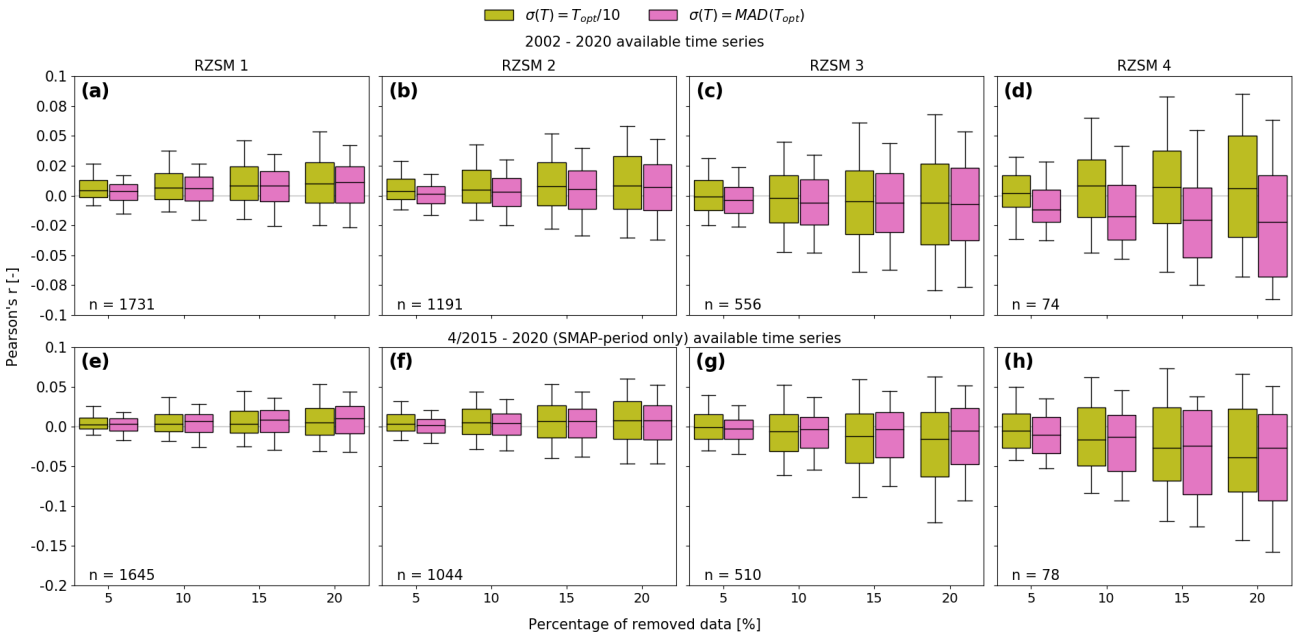

Figure 7. Correlations with in situ measurements (y axis) before and after removing a fixed percentage of data with the highest uncertainty (x axis) for the period 2002–2020 **(a–d)** and 2015–2020 **(e–h)**. Uncertainties were calculated using either $\sigma(T) = T_{\mathrm{opt}}/10$ (olive colour) or $\sigma(T) = \mathrm{MAD}(T_{\mathrm{opt}})$ (orchid colour).

in situ RZSM measurements taken at the same location and depth. This was done at all available ISMN sites, and the median of these estimates was used as a global proxy for EF structural uncertainty for each of the four product depth layers, respectively. Combined, propagated SSM input and model parameter uncertainties and EF structural uncertainties were considered to yield realistic estimates of the total RZSM product uncertainty budget in all layers (global mean uncertainties in the four product layers are 0.031, 0.035, 0.04, and 0.04 $\mathrm{m}^3\ \mathrm{m}^{-3}$). Note, however, that a quantitative validation of uncertainty magnitudes is still pending due to the lack of reliable uncertainty reference data on a global scale and for different RZSM depth layers.

The EF parameter uncertainty was estimated on a global scale and can be expected to differ for smaller scales, especially where the variability in environmental conditions is lower. Similarly, estimates of the EF model structural uncertainty are likely to differ on local to regional scales. Also, the structural uncertainty in the EF, here assumed to be constant in time, could in fact vary on a sub-seasonal scale given the phenomena that regulate the process of water transfer in the soil. Moreover, random errors in the in situ measurements were assumed to be negligible and were not accounted for in estimating the structural uncertainty in the model. Nonetheless, it is plausible that the EF structural uncertainty is much greater than the random uncertainty in the in situ sensors. Estimates of the random uncertainty in the in situ sensors could allow for a more accurate estimation of the EF structural uncertainty in the future.

Further insights could also be gained by evaluating the behaviour of the proposed method in propagating uncertainties in different SSM input data, e.g. single-sensor products without structural breaks and non-static input SSM uncertainties obtained by means other than TCA. Nonetheless, this study is an important step towards understanding and describing the uncertainties in EF-based RZSM products.

Appendix A: ISMN references

Table A1. ISMN networks used in this study. A list of all available ISMN networks can be found at https://ismn.earth/en/networks/, last access: 28 August 2023.

Network	Time series used for T-parameter optimization	Time series used for EF model structural uncertainty estimation	Reference
AMMA-CATCH	31	27	Mougin et al. (2009), Cappelaere et al. (2009), de Rosnay et al. (2009), Lebel et al. (2009), Galle et al. (2015)
ARM	90	113	Cook (2016a), Cook (2016b), Cook (2018)
AWDN	112	148	–
BIEBRZA_S-1	15	18	Musial et al. (2016)
BNZ-LTER	7	22	Van Cleve et al. (2015)
CALABRIA	12	–	Brocca et al. (2011)
CAMPANIA	1	–	Brocca et al. (2011)
COSMOS	65	2	Zreda et al. (2008), Zreda et al. (2012)
CTP-SMTMN	147	167	Yang et al. (2013)
DAHRA	4	4	Tagesson et al. (2015)
FLUXNET-AMERIFLUX	22	16	–
FMI	16	37	Ikonen et al. (2016), Ikonen et al. (2018)
FR_Aqui	28	23	Al-Yaari et al. (2018), Wigneron et al. (2018)
GROW	118	–	Xaver et al. (2020), Zappa et al. (2019), Zappa et al. (2020)
GTK	–	24	–
HiWATER_EHWSN	–	1	Kang et al. (2014), Jin et al. (2014)
HOAL	90	97	Blöschl et al. (2016), Vreugdenhil et al. (2013)
HOBE	64	60	Jensen and Refsgaard (2018), Bircher et al. (2012)
HSC_SEOLMACHEON	1	–	–
HYDROL-NET_PERUGIA	4	6	Flammini et al. (2018a), Flammini et al. (2018b), Morbidelli et al. (2011), Morbidelli et al. (2014), Morbidelli et al. (2017)
ICN	–	24	Hollinger and Isard (1994)
IIT_KANPUR	–	3	–
IMA_CAN1	9	–	Biddoccu et al. (2016), Raffelli et al. (2017), Capello et al. (2019)
IPE	1	–	Alday et al. (2020)
iRON	5	16	Osenga et al. (2019), Osenga et al. (2021)
KIHS_CMC	54	38	–
KIHS_SMC	51	32	–
LAB-net	2	1	Mattar et al. (2014), Mattar et al. (2016)
MAQU	53	62	Su et al. (2011), Dente et al. (2012)
MOL-RAO	9	10	Beyrich and Adam (2007)
MySMNet	15	11	Kang et al. (2019)
NAQU	5	31	Su et al. (2011), Dente et al. (2012)
NGARI	5	84	Su et al. (2011), Dente et al. (2012)
NVE	–	10	–

Table A1. Continued.

Network	Time series used for T-parameter optimization	Time series used for EF model structural uncertainty estimation	Reference
ORACLE	24	32	–
OZNET	101	105	Young et al. (2008), Smith et al. (2012)
PBO_H2O	115	–	Larson et al. (2008)
PTSMN	80	60	Hajdu et al. (2019)
REMEDHUS	22	–	González-Zamora et al. (2019)
RISMA	51	62	Canisius (2011), L'Heureux (2011), Ojo et al. (2015)
RSMN	13	–	–
SASMAS	27	13	Rüdiger et al. (2007)
SCAN	575	806	Schaefer et al. (2007)
SKKU	56	42	Nguyen et al. (2017)
SMN-SDR	76	127	Zhao et al. (2020), Zheng et al. (2022)
SMOSMANIA	79	66	Calvet et al. (2007), Albergel et al. (2008), Calvet et al. (2016)
SNOTEL	788	942	Leavesley et al. (2008)
SOILSCAPE	385	247	Moghaddam et al. (2010), Moghaddam et al. (2016), Shuman et al. (2010)
SWEX_POLAND	6	17	Marczewski et al. (2010)
TAHMO	68	10	–
TERENO	14	10	Zacharias et al. (2011), Bogena et al. (2012), Bogena et al. (2018), Bogena (2016)
UDC_SMOS	16	11	Loew et al. (2009), Schlenz et al. (2012)
UMBRIA	37	28	Brocca et al. (2008), Brocca et al. (2009), Brocca et al. (2011)
UMSUOL	4	6	–
USCRN	309	358	Bell et al. (2013)
USDA-ARS	4	–	Jackson et al. (2010)
VAS	1	–	–
VDS	12	8	–
WEGENERNET	1	–	Kirchengast et al. (2014), Fuchsberger et al. (2021)
WSMN	1	–	Petropoulos and McCalmont (2017)

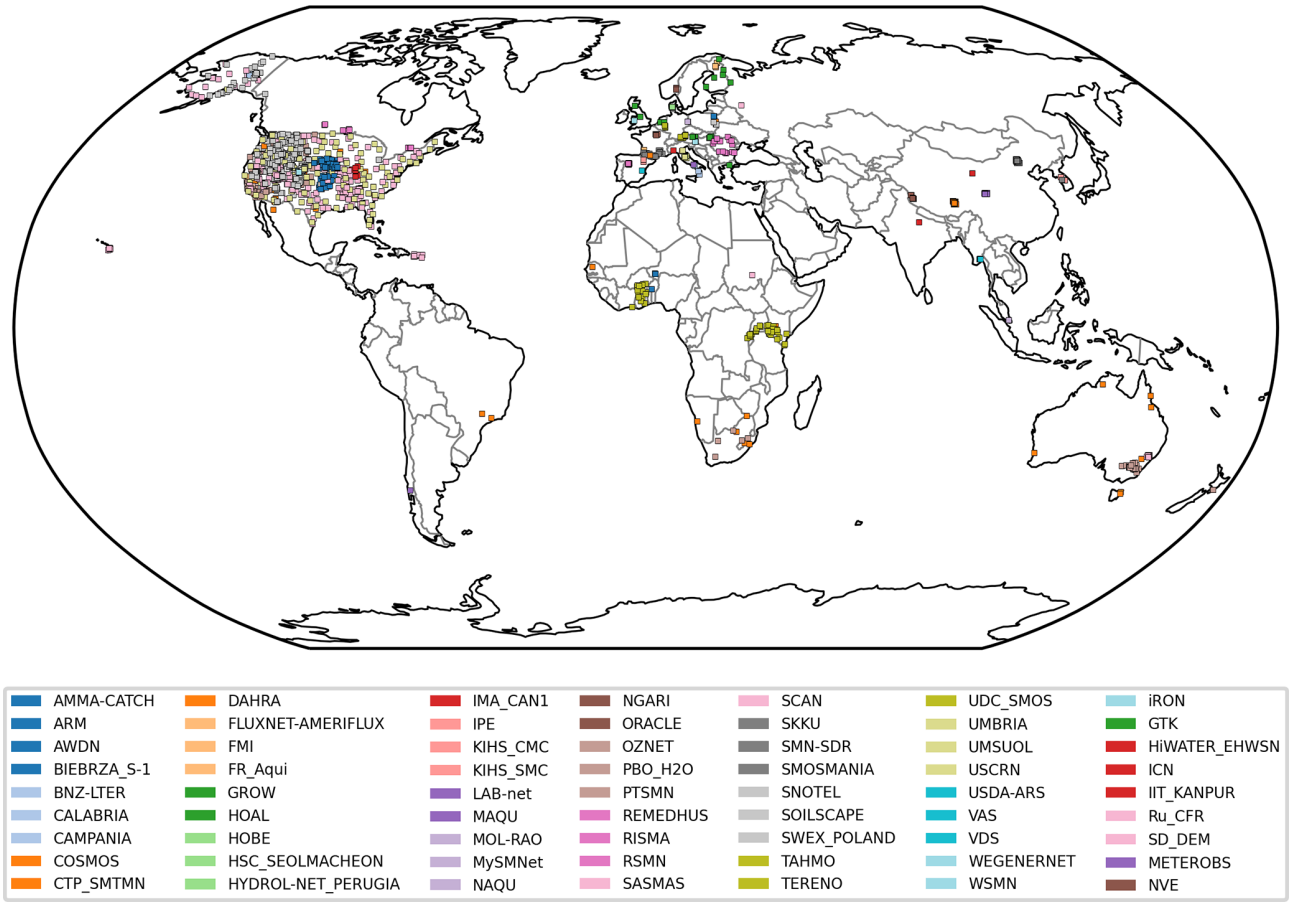

Figure A1. Location map of the ISMN in situ stations used in this study and listed in Table A1.

Code and data availability. The Python package used in the computation of the root-zone soil moisture data and their associated uncertainties from surface soil moisture observations by means of an exponential filter can be accessed here: https://doi.org/10.5281/zenodo.7534919 (Adeaem et al., 2023).

The global root-zone soil moisture data produced and utilized in this study are available for the period 2002–2020 as daily image files in netCDF4 format: https://doi.org/10.48436/9gsg6-nn854 (Pasik and Preimesberger, 2023).

Author contributions. AP: conceptualization, formal analysis, investigation, visualization, software, writing (original draft preparation). AG: conceptualization, methodology, supervision, writing (review and editing). WP: data curation, software, validation, writing (review and editing). DDS: methodology, software, writing (review and editing). WD: conceptualization, methodology, funding acquisition, supervision, writing (review and editing).

Competing interests. The contact author has declared that none of the authors has any competing interests.

Disclaimer. Publisher's note: Copernicus Publications remains neutral with regard to jurisdictional claims in published maps and institutional affiliations.

Acknowledgements. This study has been carried out as part of the Global Gravity-based Groundwater Product (G3P) project. G3P is funded in response to the Earth observation call LC-SPACE-04-EO-2019-2020 "Copernicus evolution – Research activities in support of cross-cutting applications between Copernicus services", as part of the H2020-SPACE-2018-2020 activity "Leadership in Industrial Technologies – Space Part". Please visit https://g3p.eu (last access: 28 August 2023) for further information on the project.

Financial support. This research has been supported by the European Commission, Horizon 2020 (grant no. 870353).

Review statement. This paper was edited by Hisashi Sato and reviewed by Laurène Bouaziz and one anonymous referee.

References

Adeaem, Gößwein, B., Hahn, S., Preimesberger, W., and BM, B.: TUW-GEO/pyswi: v1.0 (v1.0), Zenodo [code], https://doi.org/10.5281/zenodo.7534919, 2023.

Albergel, C., Rüdiger, C., Pellarin, T., Calvet, J.-C., Fritz, N., Froissard, F., Suquia, D., Petitpa, A., Piguet, B., and Martin, E.: From near-surface to root-zone soil moisture using an exponential filter: an assessment of the method based on in-situ observations and model simulations, Hydrol. Earth Syst. Sci., 12, 1323–1337, https://doi.org/10.5194/hess-12-1323-2008, 2008.

Al Bitar, A. and Mahmoodi, A.: Algorithm Theoretical Basis Document (ATBD) for the SMOS Level 4 Root Zone Soil Moisture (Version $v30\_01$), Tech. Rep., https://doi.org/10.5281/zenodo.4298572, 2020.

Alday, J. G., Camarero, J. J., Revilla, J., and Resco de Dios, V.: Similar diurnal, seasonal and annual rhythms in radial root expansion across two coexisting Mediterranean oak species, Tree Physiol., 40, 956–968, https://doi.org/10.1093/treephys/tpaa041, 2020.

Al-Yaari, A., Dayau, S., Chipeaux, C., Aluome, C., Kruszewski, A., Loustau, D., and Wigneron, J.-P.: The AQUI Soil Moisture Network for Satellite Microwave Remote Sensing Validation in South-Western France, Remote Sensing, 10, 1839, https://doi.org/10.3390/rs10111839, 2018.

Baldwin, D., Manfreda, S., Keller, K., and Smithwick, E.: Predicting root zone soil moisture with soil properties and satellite near-surface moisture data across the conterminous United States, J. Hydrol., 546, 393–404, https://doi.org/10.1016/j.jhydrol.2017.01.020, 2017.

Bauer Marschallinger, B.: Product User Manual CGLOPS1_PUM_SWIV3-SWI10-SWI-TS l2.60, Tech. rep., Copernicus Global Land Operations, 2018.

Bauer Marschallinger, B.: Algorithm Theoretical Basis Document, CGLOPS1_ATBD_SWI1km-V1 l1.30, Tech. rep., Copernicus Global Land Operations, 2022.

Bauer-Marschallinger, B., Paulik, C., Hochstöger, S., Mistelbauer, T., Modanesi, S., Ciabatta, L., Massari, C., Brocca, L., and Wagner, W.: Soil Moisture from Fusion of Scatterometer and SAR: Closing the Scale Gap with Temporal Filtering, Remote Sensing, 10, 1030, https://doi.org/10.3390/rs10071030, 2018.

Beck, H. E., de Jeu, R. A. M., Schellekens, J., van Dijk, A. I. J. M., and Bruijnzeel, L. A.: Improving Curve Number Based Storm Runoff Estimates Using Soil Moisture Proxies, IEEE J. Sel. Top. Appl., 2, 250–259, https://doi.org/10.1109/JSTARS.2009.2031227, 2009.

Bell, J. E., Palecki, M. A., Baker, C. B., Collins, W. G., Lawrimore, J. H., Leeper, R. D., Hall, M. E., Kochendorfer, J., Meyers, T. P., Wilson, T., and Diamond, H. J.: U.S. Climate Reference Network Soil Moisture and Temperature Observations, J. Hydrometeorol., 14, 977–988, https://doi.org/10.1175/JHM-D-12-0146.1, 2013.

Beven, K.: On the concept of model structural error, Water Sci. Technol., 52, 167–175, https://doi.org/10.2166/wst.2005.0165, 2005.

Beyrich, F. and Adam, W.: Site and Data Report for the Lindenberg Reference Site in CEOP – Phase 1, Tech. Rep. 230, Deutscher Wetterdienst, Offenbach am Main, 2007.

Biddoccu, M., Ferraris, S., Opsi, F., and Cavallo, E.: Long-term monitoring of soil management effects on runoff and soil erosion in sloping vineyards in Alto Monferrato (North–West Italy), Soil Till. Res., 155, 176–189, https://doi.org/10.1016/j.still.2015.07.005, 2016.

Bircher, S., Skou, N., Jensen, K. H., Walker, J. P., and Rasmussen, L.: A soil moisture and temperature network for SMOS validation in Western Denmark, Hydrol. Earth Syst. Sci., 16, 1445–1463, https://doi.org/10.5194/hess-16-1445-2012, 2012.

Blöschl, G., Blaschke, A. P., Broer, M., Bucher, C., Carr, G., Chen, X., Eder, A., Exner-Kittridge, M., Farnleitner, A., Flores-Orozco, A., Haas, P., Hogan, P., Kazemi Amiri, A., Oismüller, M., Parajka, J., Silasari, R., Stadler, P., Strauss, P., Vreugdenhil, M., Wagner, W., and Zessner, M.: The Hydrological Open Air Laboratory (HOAL) in Petzenkirchen: a hypothesis-driven observatory, Hydrol. Earth Syst. Sci., 20, 227–255, https://doi.org/10.5194/hess-20-227-2016, 2016.

Bogena, H., Kunkel, R., Puetz, T., Vereecken, H., Krueger, E., Zacharias, S., Dietrich, P., Wollschlaeger, U., Kunstmann, H., Papen, H., Schmid, H. P., Munch, J. C., Priesack, E., Schwank, M., Bens, O., Brauer, A., Borg, E., and Hajnsek, I.: TERENO – Long-term monitoring network for terrestrial environmental research, Hydrol. Wasserbewirts., 56, 138–143, 2012.

Bogena, H., Montzka, C., Huisman, J., Graf, A., Schmidt, M., Stockinger, M., von Hebel, C., Hendricks-Franssen, H., van der Kruk, J., Tappe, W., Lücke, A., Baatz, R., Bol, R., Groh, J., Pütz, T., Jakobi, J., Kunkel, R., Sorg, J., and Vereecken, H.: The TERENO-Rur Hydrological Observatory: A Multi-scale Multi-Compartment Research Platform for the Advancement of Hydrological Science, Vadose Zone J., 17, 180055, https://doi.org/10.2136/vzj2018.03.0055, 2018.

Bogena, H. R.: TERENO: German network of terrestrial environmental observatories, Journal of Large-Scale Research Facilities, 2, A52–A52, https://doi.org/10.17815/jlsrf-2-98, 2016.

Bouaziz, L. J. E., Steele-Dunne, S. C., Schellekens, J., Weerts, A. H., Stam, J., Sprokkereef, E., Winsemius, H. H. C., Savenije, H. H. G., and Hrachowitz, M.: Improved Understanding of the Link Between Catchment-Scale Vegetation Accessible Storage and Satellite-Derived Soil Water Index, Water Resour. Res., 56, e2019WR026365, https://doi.org/10.1029/2019WR026365, 2020.

Brocca, L., Melone, F., and Moramarco, T.: On the estimation of antecedent wetness conditions in rainfall–runoff modelling, Hydrol. Process., 22, 629–642, https://doi.org/10.1002/hyp.6629, 2008.

Brocca, L., Melone, F., Moramarco, T., and Morbidelli, R.: Antecedent wetness conditions based on ERS scatterometer data, J. Hydrol., 364, 73–87, https://doi.org/10.1016/j.jhydrol.2008.10.007, 2009.

Brocca, L., Melone, F., Moramarco, T., Wagner, W., and Hasenauer, S.: ASCAT soil wetness index validation through in situ and modeled soil moisture data in central Italy, Remote Sens. Environ., 114, 2745–2755, https://doi.org/10.1016/j.rse.2010.06.009, 2010.

Brocca, L., Hasenauer, S., Lacava, T., Melone, F., Moramarco, T., Wagner, W., Dorigo, W., Matgen, P., Martínez-Fernández, J., Llorens, P., Latron, J., Martin, C., and Bittelli, M.: Soil moisture estimation through ASCAT and AMSR-E sensors: An intercomparison and validation study across Europe, Remote Sens. Environ., 115, 3390–3408, https://doi.org/10.1016/j.rse.2011.08.003, 2011.

C3S: Algorithm Theoretical Baseline Document (ATBD) – Soil Moisture Service D1.SM.2-v3.0, Tech. Rep., EODC, https://doi.org/10.24381/cds.d7782f18, 2020.

Calvet, J.-C., Fritz, N., Froissard, F., Suquia, D., Petitpa, A., and Piguet, B.: In situ soil moisture observations for the CAL/VAL of SMOS: the SMOSMANIA network, in: 2007 IEEE International Geoscience and Remote Sensing Symposium, Barcelona, Spain, 23–28 July 2007, 1196–1199, https://doi.org/10.1109/IGARSS.2007.4423019, 2007.

Calvet, J.-C., Fritz, N., Berne, C., Piguet, B., Maurel, W., and Meurey, C.: Deriving pedotransfer functions for soil quartz fraction in southern France from reverse modeling, SOIL, 2, 615–629, https://doi.org/10.5194/soil-2-615-2016, 2016.

Canisius, F.: Calibration of Casselman, Ontario Soil Moisture Monitoring Network, Tech. Rep., Agriculture and Agri-food Canada, 2011.

Capello, G., Biddoccu, M., Ferraris, S., and Cavallo, E.: Effects of Tractor Passes on Hydrological and Soil Erosion Processes in Tilled and Grassed Vineyards, Water, 11, 2118, https://doi.org/10.3390/w11102118, 2019.

Cappelaere, B., Descroix, L., Lebel, T., Boulain, N., Ramier, D., Laurent, J.-P., Favreau, G., Boubkraoui, S., Boucher, M., Bouzou Moussa, I., Chaffard, V., Hiernaux, P., Issoufou, H., Le Breton, E., Mamadou, I., Nazoumou, Y., Oi, M., Ottlé, C., and Quantin, G.: The AMMA-CATCH experiment in the cultivated Sahelian area of south-west Niger – Investigating water cycle response to a fluctuating climate and changing environment, J. Hydrol., 375, 34–51, https://doi.org/10.1016/j.jhydrol.2009.06.021, 2009.

Cook, D. R.: Soil Water and Temperature System (SWATS) Instrument Handbook, Tech. Rep., US Department of Energy, https://doi.org/10.2172/1251383, 2016a.

Cook, D. R.: Soil Temperature and Moisture Profile (STAMP) System Handbook, Tech. Rep., US Department of Energy, https://doi.org/10.2172/1332724, 2016b.

Cook, D. R.: Surface Energy Balance System (SEBS) Instrument Handbook, Tech. Rep., US Department of Energy, https://doi.org/10.2172/1004944, 2018.

de Lange, R., Beck, R., van de Giesen, N., Friesen, J., de Wit, A., and Wagner, W.: Scatterometer-Derived Soil Moisture Calibrated for Soil Texture With a One-Dimensional Water-Flow Model, IEEE T. Geosci. Remote, 46, 4041–4049, https://doi.org/10.1109/TGRS.2008.2000796, 2008.

Dente, L., Su, Z., and Wen, J.: Validation of SMOS Soil Moisture Products over the Maqu and Twente Regions, Sensors, 12, 9965–9986, https://doi.org/10.3390/s120809965, 2012.

de Rosnay, P., Gruhier, C., Timouk, F., Baup, F., Mougin, E., Hiernaux, P., Kergoat, L., and LeDantec, V.: Multi-scale soil moisture measurements at the Gourma meso-scale site in Mali, J. Hydrol., 375, 241–252, https://doi.org/10.1016/j.jhydrol.2009.01.015, 2009.

De Santis, D. and Biondi, D.: Error Propagation from Remotely Sensed Surface Soil Moisture Into Soil Water Index Using an Exponential Filter, in: HIC 2018. 13th International Conference on Hydroinformatics, Palermo, Italy, 1–6 July 2018, edited by: Loggia, G. L., Freni, G., Puleo, V., and Marchis, M. D., vol. 3 of EPiC Series in Engineering, EasyChair, 520–525, https://doi.org/10.29007/kvhb, 2018.

Dorigo, W., Xaver, A., Vreugdenhil, M., Gruber, A., Hegyiová, A., Sanchis-Dufau, A., Zamojski, D., Cordes, C., Wagner, W., and Drusch, M.: Global Automated Quality Control of In Situ Soil Moisture Data from the International Soil Moisture Network, Vadose Zone J., 12, vzj2012.0097, https://doi.org/10.2136/vzj2012.0097, 2013.

Dorigo, W., Wagner, W., Albergel, C., Albrecht, F., Balsamo, G., Brocca, L., Chung, D., Ertl, M., Forkel, M., Gruber, A., Haas, E., Hamer, P. D., Hirschi, M., Ikonen, J., de Jeu, R., Kidd, R., Lahoz, W., Liu, Y. Y., Miralles, D., Mistelbauer, T., Nicolai-Shaw, N., Parinussa, R., Pratola, C., Reimer, C., van der Schalie, R., Seneviratne, S. I., Smolander, T., and Lecomte, P.: ESA CCI Soil Moisture for improved Earth system understanding: State-of-the art and future directions, Remote Sens. Environ., 203, 185–215, https://doi.org/10.1016/j.rse.2017.07.001, 2017.

Dorigo, W., Dietrich, S., Aires, F., Brocca, L., Carter, S., Cretaux, J.-F., Dunkerley, D., Enomoto, H., Forsberg, R., Güntner, A., Hegglin, M. I., Hollmann, R., Hurst, D. F., Johannessen, J. A., Kummerow, C., Lee, T., Luojus, K., Looser, U., Miralles, D. G., Pellet, V., Recknagel, T., Vargas, C. R., Schneider, U., Schoeneich, P., Schröder, M., Tapper, N., Vuglinsky, V., Wagner, W., Yu, L., Zappa, L., Zemp, M., and Aich, V.: Closing the Water Cycle from Observations across Scales: Where Do We Stand?, B. Am. Meteorol. Soc., 102, E1897–E1935, https://doi.org/10.1175/BAMS-D-19-0316.1, 2021a.

Dorigo, W., Himmelbauer, I., Aberer, D., Schremmer, L., Petrakovic, I., Zappa, L., Preimesberger, W., Xaver, A., Annor, F., Ardö, J., Baldocchi, D., Bitelli, M., Blöschl, G., Bogena, H., Brocca, L., Calvet, J.-C., Camarero, J. J., Capello, G., Choi, M., Cosh, M. C., van de Giesen, N., Hajdu, I., Ikonen, J., Jensen, K. H., Kanniah, K. D., de Kat, I., Kirchengast, G., Kumar Rai, P., Kyrouac, J., Larson, K., Liu, S., Loew, A., Moghaddam, M., Martínez Fernández, J., Mattar Bader, C., Morbidelli, R., Musial, J. P., Osenga, E., Palecki, M. A., Pellarin, T., Petropoulos, G. P., Pfeil, I., Powers, J., Robock, A., Rüdiger, C., Rummel, U., Strobel, M., Su, Z., Sullivan, R., Tagesson, T., Varlagin, A., Vreugdenhil, M., Walker, J., Wen, J., Wenger, F., Wigneron, J. P., Woods, M., Yang, K., Zeng, Y., Zhang, X., Zreda, M., Dietrich, S., Gruber, A., van Oevelen, P., Wagner, W., Scipal, K., Drusch, M., and Sabia, R.: The International Soil Moisture Network: serving Earth system science for over a decade, Hydrol. Earth Syst. Sci., 25, 5749–5804, https://doi.org/10.5194/hess-25-5749-2021, 2021b.

Dorigo, W., Preimesberger, W., Moesinger, L., Pasik, A., Scanlon, T., Hahn, S., Van der Schalie, R., Van der Vliet, M., De Jeu, R., Kidd, R., Rodriguez-Fernandez, N., and Hirschi, M.: ESA Soil Moisture Climate Change Initiative: COMBINED Product, Version 05.3, Centre for Environmental Data Analysis [data set], https://catalogue.ceda.ac.uk/uuid/e43aead9947549078c2d108b2c3632b2 (last access: 28 August 2023), 2021c.

Dorigo, W. A., Wagner, W., Hohensinn, R., Hahn, S., Paulik, C., Xaver, A., Gruber, A., Drusch, M., Mecklenburg, S., van Oevelen, P., Robock, A., and Jackson, T.: The International Soil Moisture Network: a data hosting facility for global in situ soil moisture measurements, Hydrol. Earth Syst. Sci., 15, 1675–1698, https://doi.org/10.5194/hess-15-1675-2011, 2011.

Famiglietti, J. S., Ryu, D., Berg, A. A., Rodell, M., and Jackson, T. J.: Field observations of soil moisture variability across scales, Water Resour. Res., 44, W01423, https://doi.org/10.1029/2006WR005804, 2008.

Flammini, A., Corradini, C., Morbidelli, R., Saltalippi, C., Picciafuoco, T., and Giráldez, J. V.: Experimental Analyses of the Evaporation Dynamics in Bare Soils under Natural Conditions, Water Resour. Manag., 32, 1153–1166, https://doi.org/10.1007/s11269-017-1860-x, 2018a.

Flammini, A., Morbidelli, R., Saltalippi, C., Picciafuoco, T., Corradini, C., and Govindaraju, R. S.: Reassessment of a semi-analytical field-scale infiltration model through experiments under natural rainfall events, J. Hydrol., 565, 835–845, https://doi.org/10.1016/j.jhydrol.2018.08.073, 2018b.

Ford, T. W., Harris, E., and Quiring, S. M.: Estimating root zone soil moisture using near-surface observations from SMOS, Hydrol. Earth Syst. Sci., 18, 139–154, https://doi.org/10.5194/hess-18-139-2014, 2014.

Fuchsberger, J., Kirchengast, G., and Kabas, T.: WegenerNet high-resolution weather and climate data from 2007 to 2020, Earth Syst. Sci. Data, 13, 1307–1334, https://doi.org/10.5194/essd-13-1307-2021, 2021.

Galle, S., Grippa, M., Peugeot, C., Bouzou Moussa, I., Cappelaere, B., Demarty, J., Mougin, E., Lebel, T., and Chaffard, V.: AMMA-CATCH a Hydrological, Meteorological and Ecological Long Term Observatory on West Africa: Some Recent Results, in: AGU Fall Meeting Abstracts, vol. 2015, GC42A–01, 2015.

GCOS: The Global Observing System for Climate: Implementation needs, World Meteorological Organization, 214, https://public.wmo.int/en/resources/library/global-observing-system-climate-implementation-needs (last access: 28 August 2023), 2016.

GCOS: The 2022 GCOS ECVs Requirements, World Meteorological Organisation, 245, https://library.wmo.int/index.php?lvl=notice_display&id=22135#.ZFzCd6VBxjs (last access: 28 August 2023), 2022.

González-Zamora, A., Sánchez, N., Pablos, M., and Martínez-Fernández, J.: CCI soil moisture assessment with SMOS soil moisture and in situ data under different environmental conditions and spatial scales in Spain, Remote Sens. Environ., 225, 469–482, https://doi.org/10.1016/j.rse.2018.02.010, 2019.

Grillakis, M. G., Koutroulis, A. G., Alexakis, D. D., Polykretis, C., and Daliakopoulos, I. N.: Regionalizing Root-Zone Soil Moisture Estimates From ESA CCI Soil Water Index Using Machine Learning and Information on Soil, Vegetation, and Climate, Water Resour. Res., 57, e2020WR029249, https://doi.org/10.1029/2020WR029249, 2021.

Gruber, A., Dorigo, W., Crow, W., and Wagner, W.: Triple Collocation-Based Merging of Satellite Soil Moisture Retrievals, IEEE T. Geosci. Remote, 55, 6780–6792, https://doi.org/10.1109/TGRS.2017.2734070, 2017.

Gruber, A., Scanlon, T., van der Schalie, R., Wagner, W., and Dorigo, W.: Evolution of the ESA CCI Soil Moisture climate data records and their underlying merging methodology, Earth Syst. Sci. Data, 11, 717–739, https://doi.org/10.5194/essd-11-717-2019, 2019.

Gruber, A., De Lannoy, G., Albergel, C., Al-Yaari, A., Brocca, L., Calvet, J.-C., Colliander, A., Cosh, M., Crow, W., Dorigo, W., Draper, C., Hirschi, M., Kerr, Y., Konings, A., Lahoz, W., McColl, K., Montzka, C., Muñoz-Sabater, J., Peng, J., Reichle, R., Richaume, P., Rüdiger, C., Scanlon, T., van der Schalie, R., Wigneron, J.-P., and Wagner, W.: Validation practices for satellite soil moisture retrievals: What are (the) errors?, Remote Sens. Environ., 244, 111806, https://doi.org/10.1016/j.rse.2020.111806, 2020.

Gupta, H. V., Kling, H., Yilmaz, K. K., and Martinez, G. F.: Decomposition of the mean squared error and NSE performance criteria: Implications for improving hydrological modelling, J. Hydrol., 377, 80–91, https://doi.org/10.1016/j.jhydrol.2009.08.003, 2009.

Hajdu, I., Yule, I., Bretherton, M., Singh, R., and Hedley, C.: Field performance assessment and calibration of multi-depth AquaCheck capacitance-based soil moisture probes under permanent pasture for hill country soils, Agr. Water Manage., 217, 332–345, https://doi.org/10.1016/j.agwat.2019.03.002, 2019.

Hollinger, S. E. and Isard, S. A.: A Soil Moisture Climatology of Illinois, J. Climate, 7, 822–833, https://doi.org/10.1175/1520-0442(1994)007<0822:ASMCOI>2.0.CO;2, 1994.

Ikonen, J., Vehviläinen, J., Rautiainen, K., Smolander, T., Lemmetyinen, J., Bircher, S., and Pulliainen, J.: The Sodankylä in situ soil moisture observation network: an example application of ESA CCI soil moisture product evaluation, Geosci. Instrum. Method. Data Syst., 5, 95–108, https://doi.org/10.5194/gi-5-95-2016, 2016.

Ikonen, J., Smolander, T., Rautiainen, K., Cohen, J., Lemmetyinen, J., Salminen, M., and Pulliainen, J.: Spatially Distributed Evaluation of ESA CCI Soil Moisture Products in a Northern Boreal Forest Environment, Geosciences, 8, 51, https://doi.org/10.3390/geosciences8020051, 2018.

Jackson, T. J., Cosh, M. H., Bindlish, R., Starks, P. J., Bosch, D. D., Seyfried, M., Goodrich, D. C., Moran, M. S., and Du, J.: Validation of Advanced Microwave Scanning Radiometer Soil Moisture Products, IEEE T. Geosci. Remote, 48, 4256–4272, https://doi.org/10.1109/TGRS.2010.2051035, 2010.

Jensen, K. H. and Refsgaard, J. C.: HOBE: The Danish Hydrological Observatory, Vadose Zone J., 17, 180059, https://doi.org/10.2136/vzj2018.03.0059, 2018.

Jin, R., Li, X., Yan, B., Li, X., Luo, W., Ma, M., Guo, J., Kang, J., Zhu, Z., and Zhao, S.: A Nested Ecohydrological Wireless Sensor Network for Capturing the Surface Heterogeneity in the Midstream Areas of the Heihe River Basin, China, IEEE Geosci. Remote S., 11, 2015–2019, https://doi.org/10.1109/LGRS.2014.2319085, 2014.

Kang, C. S., Kanniah, K. D., and Kerr, Y. H.: Calibration of SMOS Soil Moisture Retrieval Algorithm: A Case of Tropical Site in Malaysia, IEEE T. Geosci. Remote, 57, 3827–3839, https://doi.org/10.1109/TGRS.2018.2888535, 2019.

Kang, J., Li, X., Jin, R., Ge, Y., Wang, J., and Wang, J.: Hybrid Optimal Design of the Eco-Hydrological Wireless Sensor Network in the Middle Reach of the Heihe River Basin, China, Sensors, 14, 19095–19114, https://doi.org/10.3390/s141019095, 2014.

Kirchengast, G., Kabas, T., Leuprecht, A., Bichler, C., and Truhetz, H.: WegenerNet: A Pioneering High-Resolution Network for Monitoring Weather and Climate, B. Am. Meteorol. Soc., 95, 227–242, https://doi.org/10.1175/BAMS-D-11-00161.1, 2014.

Larson, K. M., Small, E. E., Gutmann, E. D., Bilich, A. L., Braun, J. J., and Zavorotny, V. U.: Use of GPS receivers as a soil moisture network for water cycle studies, Geophys. Res. Lett., 35, L24405, https://doi.org/10.1029/2008GL036013, 2008.

Leavesley, G., David, O., Garen, D., Lea, J., Marron, J., Pagano, T., Perkins, T., and Strobel, M.: A modeling framework for improved agricultural water supply forecasting, in: AGU Fall Meeting Abstracts, vol. 1, San Francisco, CA, USA, 2008.

Lebel, T., Cappelaere, B., Galle, S., Hanan, N., Kergoat, L., Levis, S., Vieux, B., Descroix, L., Gosset, M., Mougin, E., Peugeot, C., and Seguis, L.: AMMA-CATCH studies in the Sahelian region of West-Africa: An overview, J. Hydrol., 375, 3–13, https://doi.org/10.1016/j.jhydrol.2009.03.020, 2009.

Leys, C., Ley, C., Klein, O., Bernard, P., and Licata, L.: Detecting outliers: Do not use standard deviation around the mean, use absolute deviation around the median, J. Exp. Soc. Psychol., 49, 764–766, https://doi.org/10.1016/j.jesp.2013.03.013, 2013.

L'Heureux, J.: 2011 Installation Report for AAFC- SAGES Soil Moisture Stations in Kenaston, SK, Tech. Rep., Agriculture and Agri-food Canada, 2011.

Loew, A., Dall'Amico, J. T., Schlenz, F., and Mauser, W.: The Upper Danube soil moisture validation site: Measurements and activities, Earth Observation and Water Cycle Science, 674, 56, 2009.

Mahmood, R. and Hubbard, K. G.: Relationship between soil moisture of near surface and multiple depths of the root zone under heterogeneous land uses and varying hydroclimatic conditions, Hydrol. Process., 21, 3449–3462, https://doi.org/10.1002/hyp.6578, 2007.

Manfreda, S., Brocca, L., Moramarco, T., Melone, F., and Sheffield, J.: A physically based approach for the estimation of root-zone soil moisture from surface measurements, Hydrol. Earth Syst. Sci., 18, 1199–1212, https://doi.org/10.5194/hess-18-1199-2014, 2014.

Marczewski, W., Slominski, J., Slominska, E., Usowicz, B., Usowicz, J., Romanov, S., Maryskevych, O., Nastula, J., and Zawadzki, J.: Strategies for validating and directions for employing SMOS data, in the Cal-Val project SWEX (3275) for wetlands, Hydrol. Earth Syst. Sci. Discuss., 7, 7007–7057, https://doi.org/10.5194/hessd-7-7007-2010, 2010.

Martens, B., Miralles, D. G., Lievens, H., van der Schalie, R., de Jeu, R. A. M., Fernández-Prieto, D., Beck, H. E., Dorigo, W. A., and Verhoest, N. E. C.: GLEAM v3: satellite-based land evaporation and root-zone soil moisture, Geosci. Model Dev., 10, 1903–1925, https://doi.org/10.5194/gmd-10-1903-2017, 2017.

Mattar, C., Santamaría-Artigas, A., Durán-Alarcón, C., Olivera-Guerra, L., Fuster, R., and Borvarán, D.: LAB-net the first Chilean soil moisture network for remote sensing applications, in: Quantitative Remote Sensing Symposium (RAQRS), 22–26 September 2014, Torrent, Spain, P4.35, 22–26, 2014.

Mattar, C., Santamaría-Artigas, A., Durán-Alarcón, C., Olivera-Guerra, L., Fuster, R., and Borvarán, D.: The LAB-Net Soil Moisture Network: Application to Thermal Remote Sensing and Surface Energy Balance, Data, 1, 6, https://doi.org/10.3390/data1010006, 2016.

Mishra, V., Ellenburg, W. L., Markert, K. N., and Limaye, A. S.: Performance evaluation of soil moisture profile estimation through entropy-based and exponential filter models, Hydrolog. Sci. J., 65, 1036–1048, https://doi.org/10.1080/02626667.2020.1730846, 2020.

Moghaddam, M., Entekhabi, D., Goykhman, Y., Li, K., Liu, M., Mahajan, A., Nayyar, A., Shuman, D., and Teneketzis, D.: A Wireless Soil Moisture Smart Sensor Web Using Physics-Based Optimal Control: Concept and Initial Demonstrations, IEEE J. Sel. Top. Appl., 3, 522–535, https://doi.org/10.1109/JSTARS.2010.2052918, 2010.

Moghaddam, M., Silva, A., Clewley, D., Akbar, R., Hussaini, S., Whitcomb, J., Devarakonda, R., Shrestha, R., Cook, R., Prakash, G., Santhana Vannan, S., and Boyer, A.: Soil Moisture Profiles and Temperature Data from SoilSCAPE Sites, USA [data set], https://doi.org/10.3334/ORNLDAAC/1339, 2016.

Morbidelli, R., Corradini, C., Saltalippi, C., Flammini, A., and Rossi, E.: Infiltration-soil moisture redistribution under natural conditions: experimental evidence as a guideline for realizing simulation models, Hydrol. Earth Syst. Sci., 15, 2937–2945, https://doi.org/10.5194/hess-15-2937-2011, 2011.

Morbidelli, R., Saltalippi, C., Flammini, A., Rossi, E., and Corradini, C.: Soil water content vertical profiles under natural conditions: matching of experiments and simulations by a conceptual model, Hydrol. Process., 28, 4732–4742, https://doi.org/10.1002/hyp.9973, 2014.

Morbidelli, R., Saltalippi, C., Flammini, A., Cifrodelli, M., Picciafuoco, T., Corradini, C., and Govindaraju, R. S.: In situ measurements of soil saturated hydraulic conductivity: Assessment of reliability through rainfall–runoff experiments, Hydrol. Process., 31, 3084–3094, https://doi.org/10.1002/hyp.11247, 2017.

Mougin, E., Hiernaux, P., Kergoat, L., Grippa, M., de Rosnay, P., Timouk, F., Le Dantec, V., Demarez, V., Lavenu, F., Arjounin, M., Lebel, T., Soumaguel, N., Ceschia, E., Mougenot, B., Baup, F., Frappart, F., Frison, P., Gardelle, J., Gruhier, C., Jarlan, L., Mangiarotti, S., Sanou, B., Tracol, Y., Guichard, F., Trichon, V., Diarra, L., Soumaré, A., Koité, M., Dembélé, F., Lloyd, C., Hanan, N., Damesin, C., Delon, C., Serça, D., Galy-Lacaux, C., Seghieri, J., Becerra, S., Dia, H., Gangneron, F., and Mazzega, P.: The AMMA-CATCH Gourma observatory site in Mali: Relating climatic variations to changes in vegetation, surface hydrology, fluxes and natural resources, J. Hydrol., 375, 14–33, https://doi.org/10.1016/j.jhydrol.2009.06.045, 2009.

Muñoz Sabater, J.: ERA5-Land hourly data from 1981 to present, Copernicus Climate Change Service (C3S) Climate Data Store (CDS) [data set], https://doi.org/10.24381/cds.e2161bac, 2019.

Muñoz Sabater, J.: ERA5-Land hourly data from 1950 to 1980, Copernicus Climate Change Service (C3S) Climate Data Store (CDS) [data set], https://doi.org/10.24381/cds.e2161bac, 2021.

Muñoz-Sabater, J., Dutra, E., Agustí-Panareda, A., Albergel, C., Arduini, G., Balsamo, G., Boussetta, S., Choulga, M., Harrigan, S., Hersbach, H., Martens, B., Miralles, D. G., Piles, M., Rodríguez-Fernández, N. J., Zsoter, E., Buontempo, C., and Thépaut, J.-N.: ERA5-Land: a state-of-the-art global reanalysis dataset for land applications, Earth Syst. Sci. Data, 13, 4349–4383, https://doi.org/10.5194/essd-13-4349-2021, 2021.

Musial, J., Dabrowska-Zielinska, K., Kiryla, W., Oleszczuk, R., Gnatowski, T., and Jaszczynski, J.: Derivation and validation of the high resolution satellite soil moisture products: a case study of the Biebrza Sentinel-1 validation sites, Geoinformation Issues, 8, 37–53, https://doi.org/10.34867/gi.2016.4, 2016.

Nguyen, H. H., Kim, H., and Choi, M.: Evaluation of the soil water content using cosmic-ray neutron probe in a heterogeneous monsoon climate-dominated region, Adv. Water Resour., 108, 125–138, https://doi.org/10.1016/j.advwatres.2017.07.020, 2017.

Ojo, E. R., Bullock, P. R., L'Heureux, J., Powers, J., McNairn, H., and Pacheco, A.: Calibration and Evaluation of a Frequency Domain Reflectometry Sensor for Real-Time Soil Moisture Monitoring, Vadose Zone J., 14, vzj2014.08.0114, https://doi.org/10.2136/vzj2014.08.0114, 2015.

Osenga, E. C., Arnott, J. C., Endsley, K. A., and Katzenberger, J. W.: Bioclimatic and Soil Moisture Monitoring Across Elevation in a Mountain Watershed: Opportunities for Research and Resource Management, Water Resour. Res., 55, 2493–2503, https://doi.org/10.1029/2018WR023653, 2019.

Osenga, E. C., Vano, J. A., and Arnott, J. C.: A community-supported weather and soil moisture monitoring database of the Roaring Fork catchment of the Colorado River Headwaters, Hydrol. Process., 35, e14081, https://doi.org/10.1002/hyp.14081, 2021.

Parinussa, R. M., Meesters, A. G. C. A., Liu, Y. Y., Dorigo, W., Wagner, W., and de Jeu, R. A. M.: Error Estimates for Near-Real-Time Satellite Soil Moisture as Derived From the Land Parameter Retrieval Model, IEEE Geosci. Remote S., 8, 779–783, https://doi.org/10.1109/LGRS.2011.2114872, 2011.

Pasik, A. J. and Preimesberger, W.: 2002–2020 Error-characterized Root-zone Soil Moisture (0–2 m) from C3S Surface Observations (1.6), TU Wien [data set], https://doi.org/10.48436/9gsg6-nn854, 2023.

Pathe, C., Wagner, W., Sabel, D., Doubkova, M., and Basara, J.: Using ENVISAT ASAR global mode data for surface soil moisture retrieval over Oklahoma, USA, IEEE Trans. Geosci. Rem. Sens., 47, 468–480, https://doi.org/10.1109/TGRS.2008.2004711, 2009.

Paulik, C., Dorigo, W., Wagner, W., and Kidd, R.: Validation of the ASCAT Soil Water Index using in situ data from the International Soil Moisture Network, Int. J. Appl. Earth Obs., 30, 1–8, https://doi.org/10.1016/j.jag.2014.01.007, 2014.

Pellarin, T., Calvet, J.-C., and Wagner, W.: Evaluation of ERS scatterometer soil moisture products over a half-degree region in southwestern France, Geophys. Res. Lett., 33, L17401, https://doi.org/10.1029/2006GL027231, 2006.

Petropoulos, G. P. and McCalmont, J. P.: An Operational In Situ Soil Moisture & Soil Temperature Monitoring Network for West Wales, UK: The WSMN Network, Sensors, 17, 1481, https://doi.org/10.3390/s17071481, 2017.

Preimesberger, W., Scanlon, T., Su, C.-H., Gruber, A., and Dorigo, W.: Homogenization of Structural Breaks in the Global ESA CCI Soil Moisture Multisatellite Climate Data Record, IEEE T. Geosci. Remote, 59, 2845–2862, https://doi.org/10.1109/TGRS.2020.3012896, 2021.

Raffelli, G., Previati, M., Canone, D., Gisolo, D., Bevilacqua, I., Capello, G., Biddoccu, M., Cavallo, E., Deiana, R., Cassiani, G., and Ferraris, S.: Local- and Plot-Scale Measurements of Soil Moisture: Time and Spatially Resolved Field Techniques in Plain, Hill and Mountain Sites, Water, 9, 706, https://doi.org/10.3390/w9090706, 2017.

Reichle, R., DeLannoy, G., Koster, R. D., Crow, W. T., and Kimball, J.: SMAP L4 9 km EASE-Grid Surface and Root Zone Soil Moisture Geophysical Data, Version 3, Tech. Rep., TU Vienna, https://doi.org/10.5067/B59DT1D5UMB4, 2017.

Rodell, M., Houser, P. R., Jambor, U., Gottschalck, J., Mitchell, K., Meng, C.-J., Arsenault, K., Cosgrove, B., Radakovich, J., Bosilovich, M., Entin, J. K., Walker, J. P., Lohmann, D., and Toll, D.: The Global Land Data Assimilation System, B. Am. Meteorol. Soc., 85, 381–394, https://doi.org/10.1175/BAMS-85-3-381, 2004.

Rüdiger, C., Hancock, G., Hemakumara, H. M., Jacobs, B., Kalma, J. D., Martinez, C., Thyer, M., Walker, J. P., Wells, T., and Willgoose, G. R.: Goulburn River experimental catchment data set, Water Resour. Res., 43, W10403, https://doi.org/10.1029/2006WR005837, 2007.

Schaefer, G. L., Cosh, M. H., and Jackson, T. J.: The USDA Natural Resources Conservation Service Soil Climate Analysis Network (SCAN), J. Atmos. Ocean. Tech., 24, 2073–2077, https://doi.org/10.1175/2007JTECHA930.1, 2007.

Schlenz, F., dall'Amico, J. T., Loew, A., and Mauser, W.: Uncertainty Assessment of the SMOS Validation in the Upper Danube Catchment, IEEE T. Geosci. Remote, 50, 1517–1529, https://doi.org/10.1109/TGRS.2011.2171694, 2012.

Shuman, D. I., Nayyar, A., Mahajan, A., Goykhman, Y., Li, K., Liu, M., Teneketzis, D., Moghaddam, M., and Entekhabi, D.: Measurement Scheduling for Soil Moisture Sensing: From Physical Models to Optimal Control, P. IEEE, 98, 1918–1933, https://doi.org/10.1109/JPROC.2010.2052532, 2010.

Smith, A. B., Walker, J. P., Western, A. W., Young, R. I., Ellett, K. M., Pipunic, R. C., Grayson, R. B., Siriwardena, L., Chiew, F. H. S., and Richter, H.: The Murrumbidgee soil moisture monitoring network data set, Water Resour. Res., 48, W07701, https://doi.org/10.1029/2012WR011976, 2012.

Stefan, V.-G., Indrio, G., Escorihuela, M.-J., Quintana-Seguí, P., and Villar, J. M.: High-Resolution SMAP-Derived Root-Zone Soil Moisture Using an Exponential Filter Model Calibrated per Land Cover Type, Remote Sensing, 13, 1112, https://doi.org/10.3390/rs13061112, 2021.

Su, Z., Wen, J., Dente, L., van der Velde, R., Wang, L., Ma, Y., Yang, K., and Hu, Z.: The Tibetan Plateau observatory of plateau scale soil moisture and soil temperature (Tibet-Obs) for quantifying uncertainties in coarse resolution satellite and model products, Hydrol. Earth Syst. Sci., 15, 2303–2316, https://doi.org/10.5194/hess-15-2303-2011, 2011.

Sure, A. and Dikshit, O.: Estimation of root zone soil moisture using passive microwave remote sensing: A case study for rice and wheat crops for three states in the Indo-Gangetic basin, J. Environ. Manage., 234, 75–89, https://doi.org/10.1016/j.jenvman.2018.12.109, 2019.

Tagesson, T., Fensholt, R., Guiro, I., Rasmussen, M. O., Huber, S., Mbow, C., Garcia, M., Horion, S., Sandholt, I., Holm-Rasmussen, B., Göttsche, F. M., Ridler, M.-E., Olén, N., Lundegard Olsen, J., Ehammer, A., Madsen, M., Olesen, F. S., and Ardö, J.: Ecosystem properties of semiarid savanna grassland in West Africa and its relationship with environmental variability, Glob. Change Biol., 21, 250–264, https://doi.org/10.1111/gcb.12734, 2015.

Taylor, J. R.: An Introduction to Error Analysis: The Study of Uncertainties in Physical Measurements, 2nd edn., University Science Books, Sausalito, ISBN 9780935702750, 1997.

Tobin, K. J., Torres, R., Crow, W. T., and Bennett, M. E.: Multi-decadal analysis of root-zone soil moisture applying the exponential filter across CONUS, Hydrol. Earth Syst. Sci., 21, 4403–4417, https://doi.org/10.5194/hess-21-4403-2017, 2017.

Van Cleve, K., Chapin, F., Stuart, R., and W., R.: Bonanza Creek Long Term Ecological Research Project Climate Database, https://www.lter.uaf.edu/ (last access: 28 August 2023), 2015.

van der Schalie, R., de Jeu, R., Kerr, Y., Wigneron, J., Rodríguez-Fernández, N., Al-Yaari, A., Parinussa, R., Mecklenburg, S., and Drusch, M.: The merging of radiative transfer based surface soil

moisture data from SMOS and AMSR-E, Remote Sens. Environ., 189, 180–193, https://doi.org/10.1016/j.rse.2016.11.026, 2017.

Vreugdenhil, M., Dorigo, W., Broer, M., Haas, P., Eder, A., Hogan, P., Bloeschl, G., and Wagner, W.: Towards a high-density soil moisture network for the validation of SMAP in Petzenkirchen, Austria, in: 2013 IEEE International Geoscience and Remote Sensing Symposium – IGARSS, 21–26 July 2013, Melbourne, VIC, Australia, 1865–1868, https://doi.org/10.1109/IGARSS.2013.6723166, 2013.

Vreugdenhil, M., Greimeister-Pfeil, I., Preimesberger, W., Camici, S., Dorigo, W., Enenkel, M., van der Schalie, R., Steele-Dunne, S., and Wagner, W.: Microwave remote sensing for agricultural drought monitoring: Recent developments and challenges, Frontiers in Water, 4, 1045451, https://doi.org/10.3389/frwa.2022.1045451, 2022.

Wagner, W., Lemoine, G., and Rott, H.: A Method for Estimating Soil Moisture from ERS Scatterometer and Soil Data, Remote Sens. Environ., 70, 191–207, https://doi.org/10.1016/S0034-4257(99)00036-X, 1999.

Wang, T., Franz, T. E., You, J., Shulski, M. D., and Ray, C.: Evaluating controls of soil properties and climatic conditions on the use of an exponential filter for converting near surface to root zone soil moisture contents, J. Hydrol., 548, 683–696, https://doi.org/10.1016/j.jhydrol.2017.03.055, 2017.

Wigneron, J.-P., Dayan, S., Kruszewski, A., Aluome, C., Al-Yaari, M. G.-E. A., Fan, L., Guven, S., Chipeaux, C., Moisy, C., Guyon, D., and Loustau, D.: The Aqui Network: Soil Moisture Sites in the "Les Landes" Forest and Graves Vineyards (Bordeaux Aquitaine Region, France), in: IGARSS 2018–2018 IEEE International Geoscience and Remote Sensing Symposium, 22–27 July 2018, Valencia, Spain, 3739–3742, https://doi.org/10.1109/IGARSS.2018.8517392, 2018.

Xaver, A., Zappa, L., Rab, G., Pfeil, I., Vreugdenhil, M., Hemment, D., and Dorigo, W. A.: Evaluating the suitability of the consumer low-cost Parrot Flower Power soil moisture sensor for scientific environmental applications, Geosci. Instrum. Method. Data Syst., 9, 117–139, https://doi.org/10.5194/gi-9-117-2020, 2020.

Yang, K., Qin, J., Zhao, L., Chen, Y., Tang, W., Han, M., Lazhu, Chen, Z., Lv, N., Ding, B., Wu, H., and Lin, C.: A Multiscale Soil Moisture and Freeze–Thaw Monitoring Network on the Third Pole, B. Am. Meteorol. Soc., 94, 1907–1916, https://doi.org/10.1175/BAMS-D-12-00203.1, 2013.

Yang, Y., Bao, Z., Wu, H., Wang, G., Liu, C., Wang, J., and Zhang, J.: An Exponential Filter Model-Based Root-Zone Soil Moisture Estimation Methodology from Multiple Datasets, Remote Sensing, 14, 1785, https://doi.org/10.3390/rs14081785, 2022.

Young, R., Walker, J., Yeoh, N., Smith, A.and Ellett, K., Merlin, O., and Western, A.: Soil moisture and meteorological observations from the murrumbidgee catchment, Tech. Rep., Department of Civil and Environmental Engineering, The University of Melbourne, 2008.

Zacharias, S., Bogena, H., Samaniego, L., Mauder, M., Fuß, R., Pütz, T., Frenzel, M., Schwank, M., Baessler, C., Butterbach-Bahl, K., Bens, O., Borg, E., Brauer, A., Dietrich, P., Hajnsek, I., Helle, G., Kiese, R., Kunstmann, H., Klotz, S., Munch, J. C., Papen, H., Priesack, E., Schmid, H. P., Steinbrecher, R., Rosenbaum, U., Teutsch, G., and Vereecken, H.: A Network of Terrestrial Environmental Observatories in Germany, Vadose Zone J., 10, 955–973, https://doi.org/10.2136/vzj2010.0139, 2011.

Zappa, L., Forkel, M., Xaver, A., and Dorigo, W.: Deriving Field Scale Soil Moisture from Satellite Observations and Ground Measurements in a Hilly Agricultural Region, Remote Sensing, 11, 2596, https://doi.org/10.3390/rs11222596, 2019.

Zappa, L., Woods, M., Hemment, D., Xaver, A., and Dorigo, W.: Evaluation of remotely sensed soil moisture products using crowdsourced measurements, in: Eighth International Conference on Remote Sensing and Geoinformation of the Environment (RSCy2020), edited by: Themistocleous, K., Papadavid, G., Michaelides, S., Ambrosia, V., and Hadjimitsis, D. G., vol. 11524, International Society for Optics and Photonics, SPIE, 115241U, https://doi.org/10.1117/12.2571913, 2020.

Zhao, T., Shi, J., Lv, L., Xu, H., Chen, D., Cui, Q., Jackson, T. J., Yan, G., Jia, L., Chen, L., Zhao, K., Zheng, X., Zhao, L., Zheng, C., Ji, D., Xiong, C., Wang, T., Li, R., Pan, J., Wen, J., Yu, C., Zheng, Y., Jiang, L., Chai, L., Lu, H., Yao, P., Ma, J., Lv, H., Wu, J., Zhao, W., Yang, N., Guo, P., Li, Y., Hu, L., Geng, D., and Zhang, Z.: Soil moisture experiment in the Luan River supporting new satellite mission opportunities, Remote Sens. Environ., 240, 111 680, https://doi.org/10.1016/j.rse.2020.111680, 2020.

Zheng, J., Zhao, T., Lü, H., Shi, J., Cosh, M. H., Ji, D., Jiang, L., Cui, Q., Lu, H., Yang, K., Wigneron, J.-P., Li, X., Zhu, Y., Hu, L., Peng, Z., Zeng, Y., Wang, X., and Kang, C. S.: Assessment of 24 soil moisture datasets using a new in situ network in the Shandian River Basin of China, Remote Sens. Environ., 271, 112891, https://doi.org/10.1016/j.rse.2022.112891, 2022.

Zreda, M., Desilets, D., Ferré, T. P. A., and Scott, R. L.: Measuring soil moisture content non-invasively at intermediate spatial scale using cosmic-ray neutrons, Geophys. Res. Lett., 35, L21402, https://doi.org/10.1029/2008GL035655, 2008.

Zreda, M., Shuttleworth, W. J., Zeng, X., Zweck, C., Desilets, D., Franz, T., and Rosolem, R.: COSMOS: the COsmic-ray Soil Moisture Observing System, Hydrol. Earth Syst. Sci., 16, 4079–4099, https://doi.org/10.5194/hess-16-4079-2012, 2012.